[redacted] CONFIDENTIAL

Copy
RM H58B24

1543
MAY 21
TECH LIBRARY KAFB, NM
0143734

NACA RM H58B24
7061

NACA

RESEARCH MEMORANDUM

FLIGHT INVESTIGATION OF THE AERODYNAMIC FORCES ON A WING-MOUNTED EXTERNAL-STORE INSTALLATION ON THE DOUGLAS D-558-II RESEARCH AIRPLANE

By Clinton T. Johnson

High-Speed Flight Station
Edwards, Calif.

CLASSIFIED DOCUMENT

This material contains information affecting the National Defense of the United States within the meaning of the espionage laws, Title 18, U.S.C., Secs. 793 and 794, the transmission or revelation of which in any manner to an unauthorized person is prohibited by law.

NATIONAL ADVISORY COMMITTEE
FOR AERONAUTICS

WASHINGTON
May 13, 1958

CONFIDENTIAL

[redacted]

TECH LIBRARY KAFB, NM
0143734

NATIONAL ADVISORY COMMITTEE FOR AERONAUTICS

RESEARCH MEMORANDUM

FLIGHT INVESTIGATION OF THE AERODYNAMIC FORCES ON A WING-MOUNTED EXTERNAL-STORE INSTALLATION ON THE DOUGLAS D-558-II RESEARCH AIRPLANE

By Clinton T. Johnson

SUMMARY

Aerodynamic forces have been determined for an external-store installation on the Douglas D-558-II research airplane. The store-pylon, pylon-alone, and fin loads were determined during angle-of-attack and angle-of-sideslip maneuvers over the Mach number range from 0.50 to 1.03. Wing-panel loads were determined for both the clean-wing configuration and the store configuration.

The side forces acting on the store-pylon indicate a linear variation with sideslip angle, and the resulting forces appear to be greater than comparable side forces due to angle of attack. Wing flow-separation effects at the higher angles of attack modify the local flow field, resulting in nonlinear variations of the forces acting on the store-pylon and pylon-alone.

The addition of the store body causes large increases in the side forces and moments over the angle-of-attack range, while the normal forces and moments show a similar increase only at the higher angles of attack. Coincident with the nonlinear variation of forces, an abrupt movement of the centers of pressure of the additional airload occurs on the store-pylon configuration.

The individual fins show large differences in load, indicating that the fin load depends primarily on the specific location of the fins on the store body.

The analysis of the aerodynamic loads measured on the wing panel indicates that the loads and centers of pressure of the additional airloads are generally unaffected by the addition of the pylon and the store body.

AFMDC D/S '58-36811

INTRODUCTION

For most of the operational aircraft of today the design of external-store installations has been hampered by the lack of full-scale data covering the factors influencing critical loading on a store. The difficulties encountered in the calculation of these factors at transonic speeds have placed a great deal of emphasis on the evaluation of flight test data in this speed regime.

With the anticipation of future problems in the field of external-store loads the NACA initiated a research program to investigate the effects of external stores on aircraft performance and the interference effects associated with external-store installations. References 1 to 10 represent a cross section of NACA research employing wind tunnels, flight tests, and theoretical approaches to provide basic data relevant to the external-stores problem. The present paper is concerned with the evaluation of the external-store and wing loads on the D-558-II airplane with pylon-mounted, DAC (Douglas Aircraft Co., Inc.) shape, 150-gallon fuel tanks installed at 61-percent semispan. The flight test program encompassed the Mach number range from $M = 0.50$ to $M = 1.03$ in maneuvers covering the angle-of-attack and angle-of-sideslip capabilities of the airplane. The flight program on the D-558-II research airplane was carried out at the NACA High-Speed Flight Station at Edwards, Calif.

SYMBOLS

b_w wing-panel span, ft

C_{b_w} wing-panel bending-moment coefficient, $\frac{M_b}{qS_w b_w}$

C_l external-store and pylon rolling-moment coefficient about strain-gage station $0.264h_s$ below wing-chord plane, $\frac{M_X}{qS_F l_s}$

C_m external-store and pylon pitching-moment coefficient about strain-gage station at $0.495l_s$, $\frac{M_Y}{qS_F l_s}$

C_N external-store and pylon normal-force coefficient, $\frac{F_N}{qS_F}$

C_{N_w} wing-panel normal-force coefficient

$\frac{dC_N}{d\alpha}$ external-store and pylon normal-force-coefficient slope, per degree angle of attack

$\frac{dC_N}{d\beta}$ external-store and pylon normal-force-coefficient slope, per degree angle of sideslip

$\frac{dC_{N_w}}{d\alpha}$ left wing-panel normal-force-coefficient slope, per degree angle of attack

C_n external-store and pylon yawing-moment coefficient about strain-gage station at $0.495l_s$, $\frac{M_Z}{qS_F l_s}$

C_Y external-store and pylon side-force coefficient, $\frac{F_Y}{qS_F}$

$\frac{dC_Y}{d\alpha}$ external-store and pylon side-force-coefficient slope, per degree angle of attack

$\frac{dC_Y}{d\beta}$ external-store and pylon side-force-coefficient slope, per degree angle of sideslip

c wing chord, ft

$\bar{c}_w$ wing-panel mean aerodynamic chord, ft

F_N external-store and pylon normal force, lb

F_Y external-store and pylon side force, lb

h_s store height, distance below wing-chord plane to center line of store body at pylon strain-gage station, in.

L_f external-store fin shear load, lb

l_s external-store length, in.

M free-stream Mach number

[redacted]

[redacted]

M_b wing-panel bending moment, in-lb

M_{b_f} external-store fin bending moment, in-lb

M_X external-store and pylon rolling moment about pylon strain-gage station, in-lb

M_Y external-store and pylon pitching moment about pylon strain-gage station, in-lb

M_Z external-store and pylon yawing moment about pylon strain-gage station, in-lb

q free-stream dynamic pressure, lb/sq ft

S_F maximum frontal area of store body, 2.4 sq ft

S_w wing-panel area, sq ft

$(x_{cp})_N$ longitudinal center of pressure of additional airload on external store and pylon due to normal force, $\left[0.495 - \left(dC_m/dC_N\right)\right] 100$, percent of store length aft of store nose

$(x_{cp})_Y$ longitudinal center of pressure of additional airload on external store and pylon due to side force, $\left[0.495 - \left(dC_n/dC_Y\right)\right] 100$, percent of store length aft of store nose

$(x_{cp})_w$ left wing-panel longitudinal center of pressure of additional airload, $\left(0.25 - C_{m_{\bar{c}_w/4}}/C_{N_w}\right)$, percent $\bar{c}_w$

$(y_{cp})_w$ left wing-panel spanwise center of pressure of additional airload, $\left(C_{b_w}/C_{N_w}\right)$, percent b_w

z_{cp} vertical center of pressure of the additional airload on external store and pylon due to side force, $\left[0.264 - l_s/h_s\left(dC_l/dC_Y\right)\right] 100$, percent h_s

α airplane angle of attack, deg

β airplane angle of sideslip, deg

[redacted]

[redacted]

TEST APPARATUS

Airplane and External-Store Arrangement

The Douglas D-558-II airplane used in this investigation is a swept-wing research airplane. Photographs of the airplane are shown in figure 1, and a three-view drawing is shown in figure 2. Table I presents physical characteristics of the airplane.

The D-558-II airplane is carried aloft in a Boeing B-29 airplane from which it is air-launched, using a rocket engine and a turbojet engine to accelerate to transonic speeds.

For the current series of tests the D-558-II was flown with two 150-gallon, DAC-shape, external stores. The stores were of 8.57 fineness ratio and were mounted at the 61-percent-semispan station on 7.5-percent-thick, sweptforward, symmetrical airfoil pylons. The store and pylon dimensions are presented in tables II and III.

The standard fin configuration of the 150-gallon tank was modified to provide adequate ground clearance when the D-558-II was mounted in the B-29 mother airplane. The fin configuration consisted of one vertical fin and two horizontal fins, as shown in figure 3(a). All flights were conducted with the stores empty.

INSTRUMENTATION AND ACCURACY

Standard NACA recording instruments were installed to measure the following quantities pertinent to this investigation:

Airspeed and altitude
Angle of attack and sideslip
Normal and transverse acceleration
Pitching, yawing, and rolling velocities and accelerations
Control positions

Shear, bending moment, and torque of the left wing panel were measured by strain gages at a root station 3 inches outboard of the wing-fuselage juncture.

The forces and moments on the left-wing store-pylon combination were measured by strain gages installed on the pylon adapter unit below the wing-pylon attachment point. Fin loads and moments were measured by strain gages mounted externally at the base of each fin. Figures 3(a)

and 3(b) show the location of the strain-gage stations. The electrical outputs of the strain-gage bridges were recorded on a multichannel oscillograph.

The results of the static calibration of the strain-gage installation for measurement of the forces and moments on the store-pylon combination and fins indicate that the following tabulated values are representative of the accuracy of the flight test data:

F_N, F_Y, lb	±30
M_X, M_Y, M_Z, in-lb	±500
L_f, lb	±15
M_{b_f}, in-lb	±100

The measured forces and moments have been corrected for inertia effects and, as presented, represent the aerodynamic loads.

The possible error in Mach number is ±0.01 at $M < 0.80$ and increases to about ±0.02 at $M \approx 0.95$. The estimated accuracy in normal and transverse acceleration is on the order of ±0.02g. Angle of attack and angle of sideslip were measured by vanes located on the nose boom and are not corrected for upwash effects or angular velocities.

FLIGHT TESTS

Flight test maneuvers were performed at altitudes between 25,000 and 35,000 feet and covered a Mach number range from stall speeds to a Mach number slightly greater than 1.00.

The airplane was tested (1) in the clean condition, (2) with pylons, and (3) with external stores attached to the pylons.

To determine the effect of angle of attack on the wing loads and store-pylon loads, wind-up-turn maneuvers were performed from trim lift with gradually increasing normal acceleration and angle of attack. The maneuver was limited by the onset of mild buffet, or normal acceleration of approximately 3g, whichever occurred first. In the transonic speed range, decreased elevator effectiveness became the primary factor limiting the magnitude of angle of attack obtained. Small sideslip angles of approximately 1° left were measured in trimmed flight. This sideslip remained essentially constant with increasing angle of attack.

To investigate the effect of sideslip on the store-pylon loads, flight maneuvers were performed which consisted of gradually increasing

right and left sideslip angles. The maneuvers were performed with wings held level at trim lift coefficient for each Mach number tested. The magnitude of maximum sideslip angle obtained during these maneuvers decreased at higher Mach numbers because of decreasing rudder effectiveness and increasing directional stability.

All maneuvers were performed by gradually increasing angle of attack or sideslip to minimize the effects of angular velocities and accelerations on the loads measurements.

RESULTS AND DISCUSSION

Side-Force Coefficients

Figure 4 shows the variation with angle of attack and angle of sideslip of the side-force coefficients for the store-pylon and pylon-alone configurations at several selected Mach numbers during angle-of-attack maneuvers and steady sideslip.

The important characteristic immediately apparent from this figure is the large effect on side force that results from the attachment of the store to the pylon. The side-force variation with either angle of attack or angle of sideslip is increased 4 to 5 times by the addition of the store. The large side-force increment in angle-of-attack maneuvers is attributed to the strong, lift-induced, spanwise flow field (ref. 7). For the sideslip maneuvers a combination of lift-induced spanwise flow at trim lift and the flow angularity created by sideslipping accounts for the large side-force increments.

The side-force-coefficient variations with angle of attack are linear at the lower angles of attack. The curves show a trend to become nonlinear at the higher angles of attack with some indication of a decrease in slope, particularly at the lower Mach numbers. The variations with angle of sideslip are essentially linear over the range of sideslip angles investigated.

The occurrence of the nonlinearity in the side-force variation at the higher angles of attack correlates approximately with the angle-of-attack boundary for decreased stability reported previously in reference 1. Reference 2, which presents the wing pressure distribution for the D-558-II airplane, indicates that wing flow separation occurs in this same angle-of-attack region. The flow-separation pattern starts at the wing tip and moves progressively inboard with increasing angle of attack. The onset of wing flow separation would be expected to alter the flow field near the wing and, therefore, would result in the nonlinear side-force variation with angle of attack shown in figure 4. Wind-tunnel

data, presented in reference 3 for a store body installed beneath a swept wing, show the same trends presented in this paper.

Normal-Force Coefficients

The variation with angle of attack and sideslip of the aerodynamic normal-force coefficients acting on the store-pylon and pylon-alone combinations is presented in figure 5. These data were obtained from the same maneuvers as were used to derive the side-force data shown in figure 4. Generally, the normal forces measured on the store-pylon and pylon-alone are lower than the side forces.

In the lower angle-of-attack region the normal-force coefficients for the store-pylon and pylon-alone are essentially linear with angle of attack. Throughout this region a slight down-load exists for both the store-pylon and pylon-alone configuration. At the higher angles of attack the normal load for the store-pylon configuration changes rather abruptly to an up-load, and the pylon-alone configuration exhibits some nonlinear characteristics. The angle of attack for these nonlinearities generally correlates with the onset of flow separation on the wing, which was discussed earlier in connection with the side forces. It appears that the flow characteristics, which govern the normal forces, are considerably modified at the higher angles of attack.

The normal-force-coefficient variations with angle of sideslip are generally linear over the angle-of-sideslip range for both configurations.

As right sideslip increases, the down-load on the store-pylon becomes greater as a result of the increased outward flow around the pylon and store.

External-Store-Load Parameters

Load-curve slopes.- The variations with Mach number of the side-force-coefficient and normal-force-coefficient slopes are summarized in figure 6. The slopes were derived from plots similar to those shown in figures 4 and 5. It should be noted that the slopes were taken only in the initial region of linear load variation with angle of attack and over the entire range of sideslip angle.

This figure illustrates the large increase in side force per degree angle of attack or sideslip caused by the addition of the store body to the pylon. For the pylon-alone configuration the effects of angle of attack and angle of sideslip are approximately equal and are essentially constant with Mach number. With the store installed, the side force per

degree sideslip is higher than the side force per degree angle of attack; this is particularly noticeable in the subsonic speed regions. At transonic speeds some variations with Mach number are apparent.

The store-pylon normal-force-coefficient slopes are generally much lower in magnitude than the side-force-coefficient slopes. The store-pylon normal-force-coefficient slopes due to either angle of attack or sideslip are approximately equal in magnitude at subsonic Mach numbers and are essentially constant with Mach number. The normal-force-coefficient slopes, derived from angle-of-attack maneuvers, indicate a slight increase in the transonic region, whereas slopes derived from sideslips remain constant. The pylon-alone normal-force-coefficient slopes derived from sideslips are near zero over the Mach number range. The angle-of-attack maneuvers produced slightly larger slopes for the pylon-alone and are about the same magnitude as the store-pylon slopes in the subsonic speed region.

Airload moments and centers of pressure.- The variations of the store-pylon and pylon-alone moments with their respective forces are presented in figures 7 to 9. It may be noted that nonlinear moment variations with forces are apparent in the data resulting from changes in angle of attack. These nonlinearities correlate with the nonlinear variation of the respective force coefficients (compare fig. 4(a) with 8(a) and figure 5(a) with 9(a)). This change in slope also indicates a rather abrupt movement of the store-pylon load centers, particularly noticeable in the movement of the longitudinal center of pressure due to side force (fig. 8(a)). It can be seen that the variations of moment coefficients with respect to force coefficients in sideslips are linear over the range of these tests.

Summary plots showing the location of the center of pressure of the additional airload of the store-pylon and pylon-alone, obtained by taking slopes of the data of figures 7 to 9 and similar variations at other Mach numbers, are shown in figure 10.

With the addition of the store body to the pylon a pronounced change in the location of the vertical center of pressure is indicated. For both configurations, sideslip maneuvers position the vertical center of pressure closer to the wing-chord plane than comparable angle-of-attack maneuvers. It may be noted, for reference, that the store-pylon juncture is approximately 60 percent of the store height below the wing-chord plane.

The longitudinal centers of pressure due to side force are essentially constant near 40 percent of the store length, regardless of Mach number, angle-of-attack, or sideslip effects.

[redacted]

The longitudinal centers of pressure due to normal force for the pylon-alone configuration are constant with Mach number at the 50-percent store-length position. The addition of the store generally moves the longitudinal center of pressure to a position rearward of the store midpoint. Angle-of-attack maneuvers show a gradually increasing rearward movement of the center of pressure with increasing Mach number, while the corresponding sideslip maneuvers show a gradual forward movement.

External-Store Fin Loads

The normal force and bending moments measured on the left store fins are presented as variations with angle of attack and sideslip in figure 11. Inasmuch as normal forces were not measured on the right horizontal fin, only bending moments are presented.

The fin-load variations indicate that the characteristics are similar to the store-pylon loads, in that the fin loads exhibit nonlinearities with respect to angle of attack and are linear with respect to sideslip angle. It is apparent that the previously discussed flow-separation effects which produce nonuniform flow fields acting on the store-pylon equally affect the fin loads. A comparison of the individual fin loads shows relatively large unsymmetrical loads. This asymmetry of load suggests that an individual fin load is largely influenced by the orientation of a fin in the local flow field around the store body.

Wing-Panel Aerodynamic Loads

The aerodynamic loads measured at the root of the wing panel are summarized in figure 12 as the variations with Mach number of lift-curve slopes and centers of pressure of the additional airload. The data presented show that the addition of the external store has relatively little effect on the wing-load characteristics. Unpublished theoretical calculations show that store-interference effects modify the span-load distribution adjacent to the store location, while the total load remains practically unchanged. The results presented in reference 1 indicate that the handling characteristics were relatively unaffected by the addition of the external stores.

CONCLUSIONS

The results of the flight test investigation of the aerodynamic loads on an external store and pylon installed on the Douglas D-558-II research airplane have shown that:

1. The side forces acting on the store and pylon vary linearly with increasing sideslip angle.

2. The side forces on the store-pylon due to angle of attack were slightly less than the side force due to sideslip angle.

3. At high angles of attack wing flow separation modifies the local flow field, which results in a nonlinear variation of the side forces and normal forces acting on the store and pylon.

4. The addition of the store body to the pylon causes large increases in the side forces and moments. The normal forces show a similar increment in force acting on the store-pylon at higher angles of attack.

5. Abrupt movements of the centers of pressure of the additional airload on the store-pylon occur near the region of nonlinear force variations with angle of attack.

6. The large differences in individual fin loads indicate that the load on an external-store fin depends primarily on the individual orientation of the fin on the store body.

7. The wing-panel load parameters were generally unaffected by the addition of the external store and pylon.

High-Speed Flight Station,
National Advisory Committee for Aeronautics,
Edwards, Calif., February 10, 1958.

REFERENCES

1. Fischel, Jack, Darville, Robert W., and Reisert, Donald: Effects of Wing-Mounted External Stores on the Longitudinal and Lateral Handling Qualities of the Douglas D-558-II Research Airplane. NACA RM H57H12, 1957.

2. Taillon, Norman V.: An Analysis of Surface Pressures and Aerodynamic Load Distribution Over the Swept Wing of the Douglas D-558-II Research Airplane at Mach Numbers From 0.73 to 1.73. NACA RM H58A30, 1958.

3. Guy, Lawrence D., and Hadaway, William M.: Aerodynamic Loads on an External Store Adjacent to a 45° Sweptback Wing at Mach Numbers From 0.70 to 1.96, Including an Evaluation of Techniques Used. NACA RM L55H12, 1955.

4. Alford, William J., Jr.: Effects of Wing-Fuselage Flow Fields on Missile Loads at Subsonic Speeds. NACA RM L55E10a, 1955.

5. Smith, Norman F., and Carlson, Harry W.: Some Effects of Configuration Variables on Store Loads at Supersonic Speeds. NACA RM L55E05, 1955.

6. Guy, Lawrence D.: Loads on External Stores at Transonic and Supersonic Speeds. NACA RM L55E13b, 1955.

7. Alford, William J., Jr.: Theoretical and Experimental Investigation of the Subsonic-Flow Fields Beneath Swept and Unswept Wings With Tables of Vortex-Induced Velocities. NACA TN 3738, 1956.

8. Nugent, Jack: Effect of Wing-Mounted External Stores on the Lift and Drag of the Douglas D-558-II Research Airplane at Transonic Speeds. NACA RM H57E15a, 1957.

9. O'Bryan, Thomas C.: Flight Measurement of Aerodynamic Loads and Moments on an External Store Mounted Under the Wing of a Swept-Wing Fighter-Type Airplane. NACA RM L53G22, 1953.

10. Hamer, Harold A., and O'Bryan, Thomas C.: Flight Measurements of the Loads and Moments on an External Store Mounted Under the Wing of a Swept-Wing Fighter-Type Airplane During Yawing and Rolling Maneuvers. NACA RM L55G22, 1955.

[redacted]

TABLE I.- PHYSICAL CHARACTERISTICS OF THE DOUGLAS D-558-II AIRPLANE

Wing:	
Root airfoil section (normal to 30-percent chord of unswept panel)	NACA 63-010
Tip airfoil section (normal to 30-percent chord of unswept panel)	NACA 63_1-012
Total area, sq ft	175
Span, ft	25
Mean aerodynamic chord, in.	87.301
Root chord (parallel to plane of symmetry), in.	108.51
Extended tip chord (parallel to plane of symmetry), in.	61.18
Taper ratio	0.565
Aspect ratio	3.570
Sweep at 30-percent chord of unswept panel, deg	35
Sweep of leading edge, deg	38.8
Incidence at fuselage center line, deg	3
Dihedral, deg	-3
Geometric twist, deg	0
Total aileron area (rearward of hinge line), sq ft	9.8
Aileron travel (each), deg	±15
Total flap area, sq ft	12.58
Flap travel, deg	50
Wing panel:	
Area, sq ft	127.6
Span, ft	19.5
Mean aerodynamic chord, in.	81.334
Horizontal tail:	
Root airfoil section (normal to 30-percent chord of unswept panel)	NACA 63-010
Tip airfoil section (normal to 30-percent chord of unswept panel)	NACA 63-010
Total area, sq ft	39.9
Span, in.	143.6
Mean aerodynamic chord, in.	41.75
Root chord (parallel to plane of symmetry), in.	53.6
Extended tip chord (parallel to plane of symmetry), in.	26.8
Taper ratio	0.50
Aspect ratio	3.59
Sweep at 30-percent chord line of unswept panel, deg	40
Dihedral, deg	0
Elevator area, sq ft	9.4
Elevator travel, deg	
Up	25
Down	15

TABLE I.- PHYSICAL CHARACTERISTICS OF THE DOUGLAS D-558-II AIRPLANE - Concluded

Vertical tail:	
Airfoil section (normal to 30-percent chord of unswept panel)	NACA 63-010
Area, sq ft	36.6
Height from fuselage center line, in.	98
Root chord (parallel to fuselage center line), in.	146
Tip chord (parallel to fuselage center line), in.	44
Sweep angle at 30-percent chord of unswept panel, deg	49
Rudder area (rearward of hinge line), sq ft	6.15
Rudder travel, deg	±25
Fuselage:	
Length, ft	42
Maximum diameter, in.	60
Fineness ratio	8.40
Speed-retarder area, sq ft	5.25
Engines:	
Turbojet	J-34-WE-40
Rocket	LR8-RM-6
Airplane weight, lb:	
Full jet and rocket fuel	15,131
Full jet fuel	11,942
No fuel	10,382
Center-of-gravity locations, percent mean aerodynamic chord:	
Full jet and rocket fuel (gear up)	23.5
Full jet fuel (gear up)	25.2
No fuel (gear up)	27
No fuel (gear down)	26.4

TABLE II.- DIMENSIONS OF 150-GALLON DOUGLAS FUEL TANK

[Stations and radii given in inches]

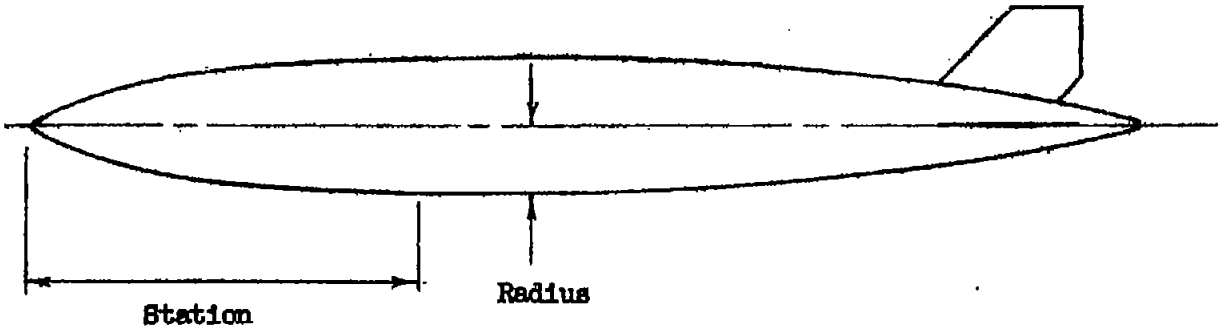

Station	Radius	Station	Radius
0	0	109.5	9.91
6	2.75	119.5	9.23
13.5	5.17	129.5	8.32
23.5	7.23	139.5	7.24
33.5	8.54	148.0	6.22
43.5	9.49	153.0	5.58
53.5	10.19	158.0	4.92
63.5	10.50	163.0	4.25
73.5	10.50	168.5	3.50
83.5	10.50	172.5	2.93
89.5	10.50	176.5	2.17
99.5	10.35	180.0	0
L.E. radius: 1.00 T.E. radius: 1.00			

TABLE III.- CROSS-SECTIONAL DIMENSIONS OF PYLON

[Stations and ordinates given in inches]

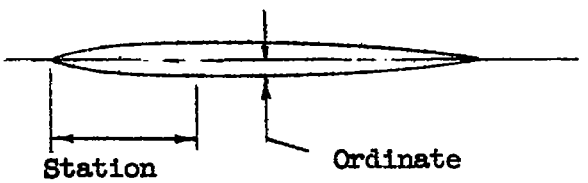

Station	Ordinate	Station	Ordinate
0	0	30.0	2.50
.5	.51	32.5	2.50
1.0	.72	38.5	2.50
2.5	1.11	41.0	2.48
5.0	1.53	43.5	2.42
7.5	1.82	46.0	2.31
10.0	2.04	48.5	2.15
12.5	2.21	51.0	1.94
15.0	2.34	53.5	1.68
17.5	2.43	58.5	1.05
20.0	2.48	63.5	.34
22.5	2.50	66.0	0
25.0	2.50		
27.5	2.50		

L.E. radius: 0.275
T.E. radius: 0.045

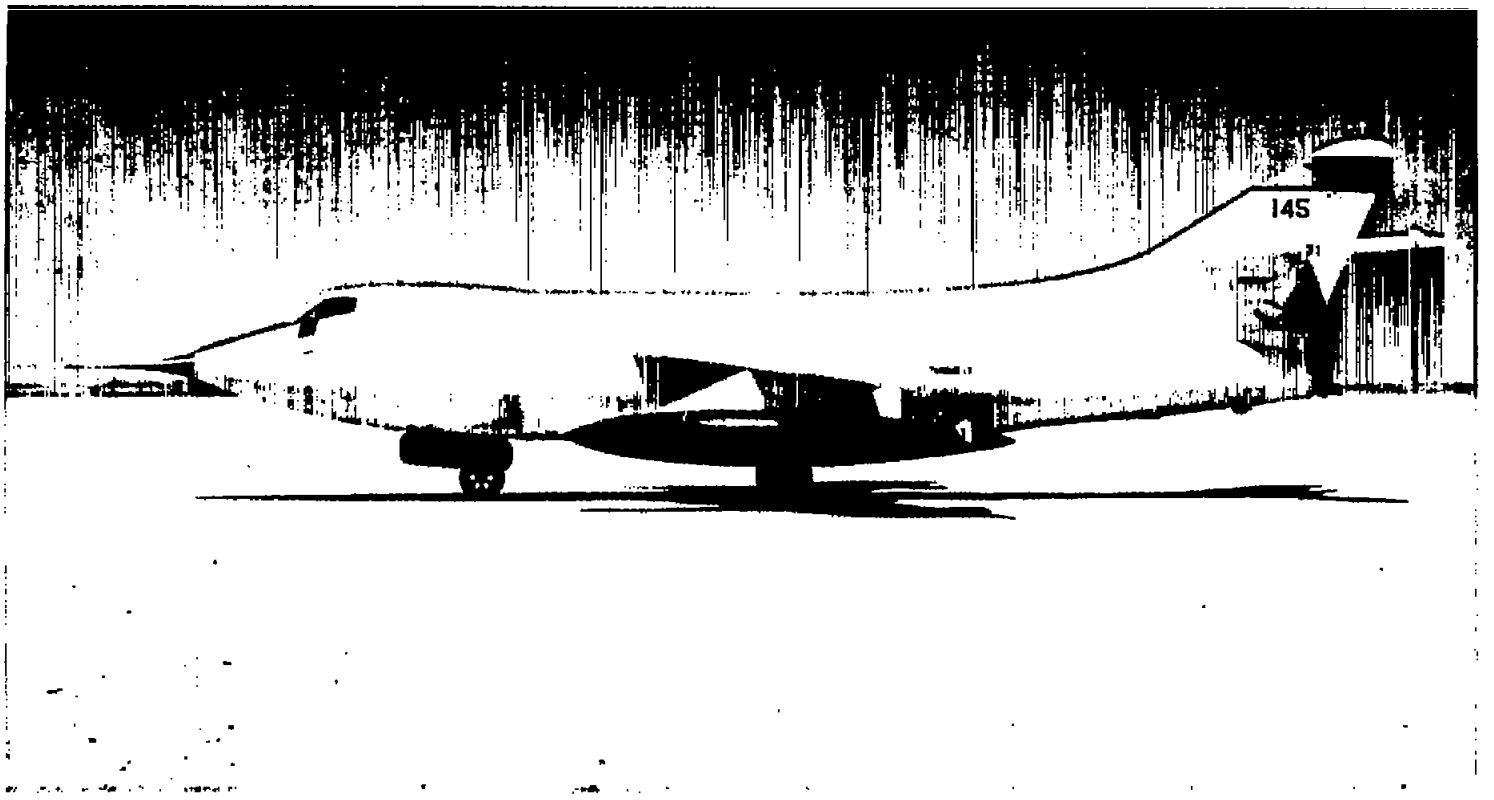

(a) Side view. E-1861

Figure 1.- Photographs of the Douglas D-558-II research airplane with DAC 150-gallon external stores.

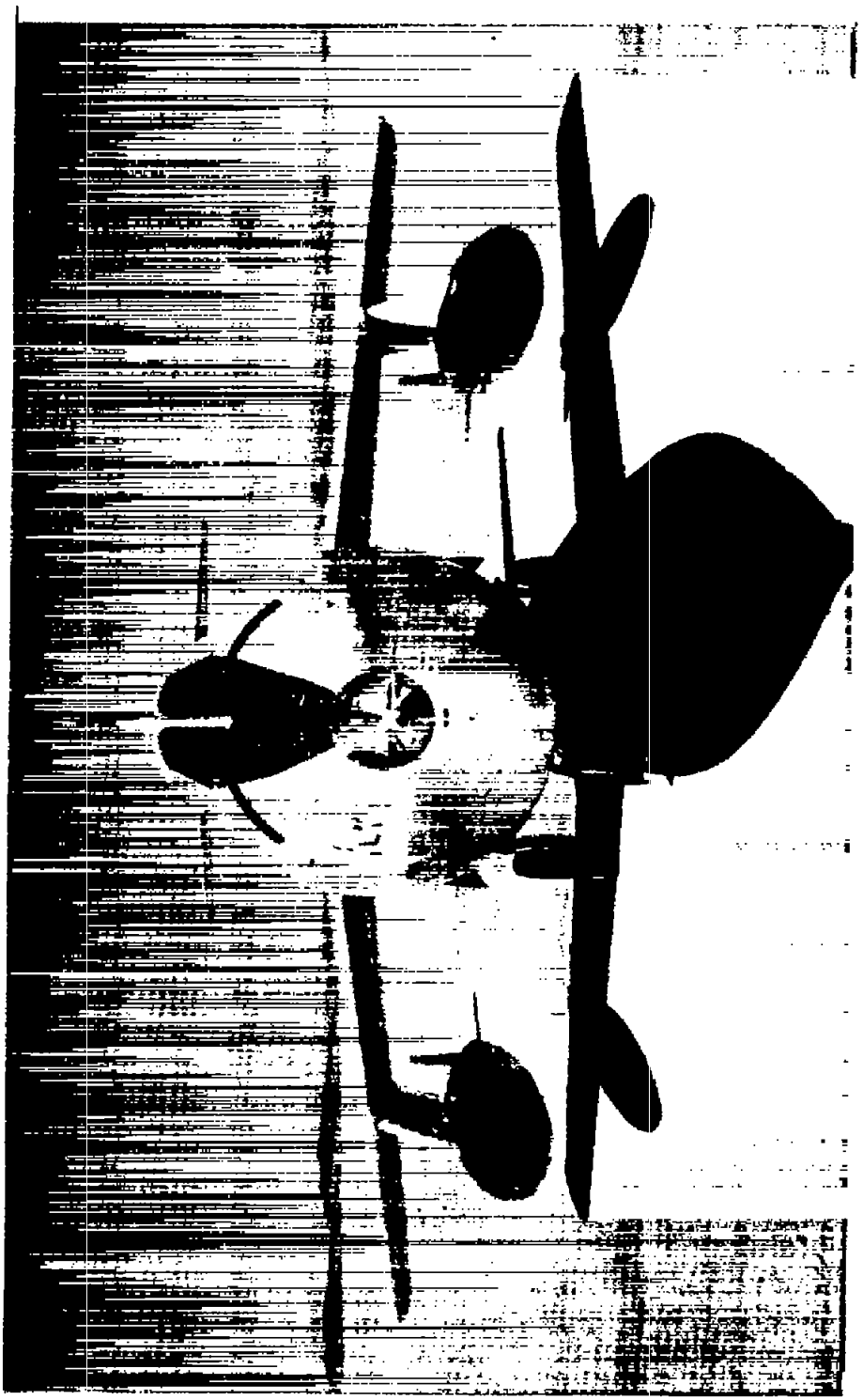

E-1859

(b) Front view.

Figure 1.- Continued.

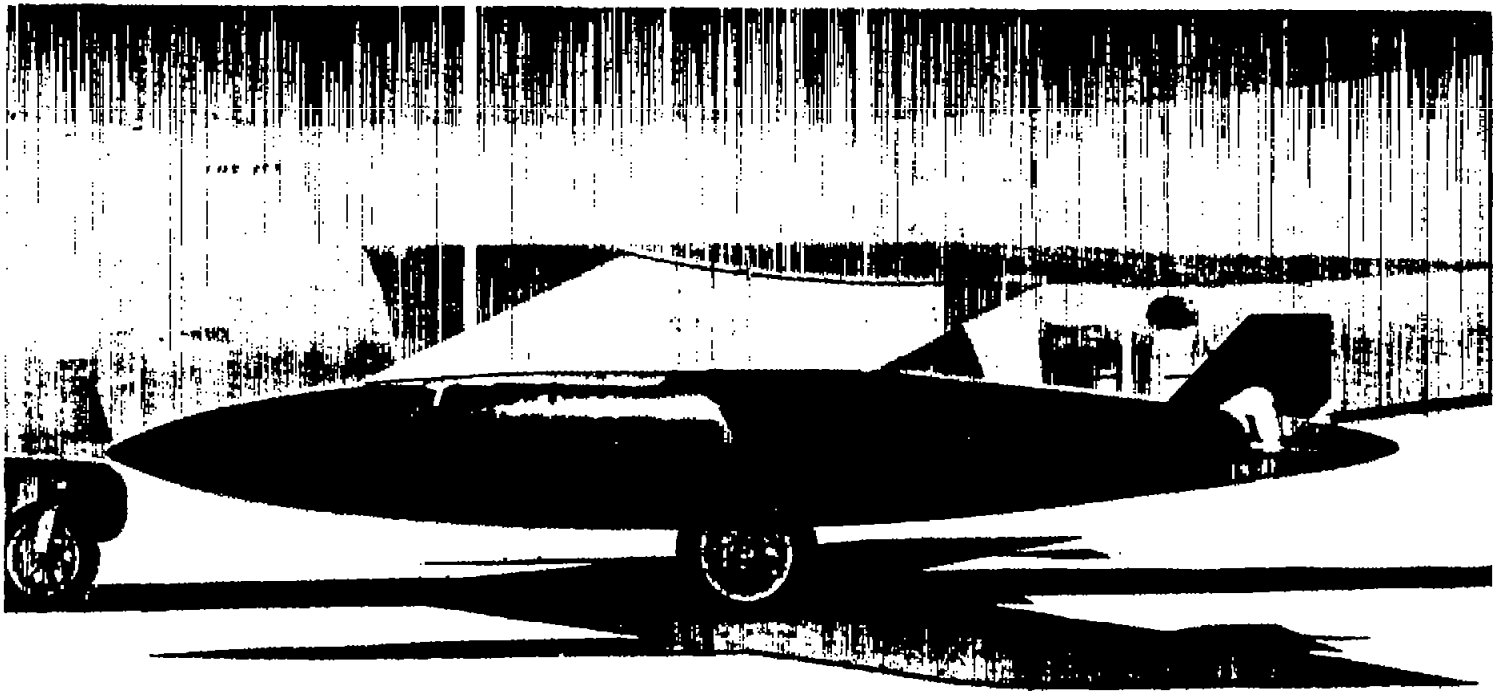

(c) Closeup view of the store. E-1867

Figure 1.- Concluded.

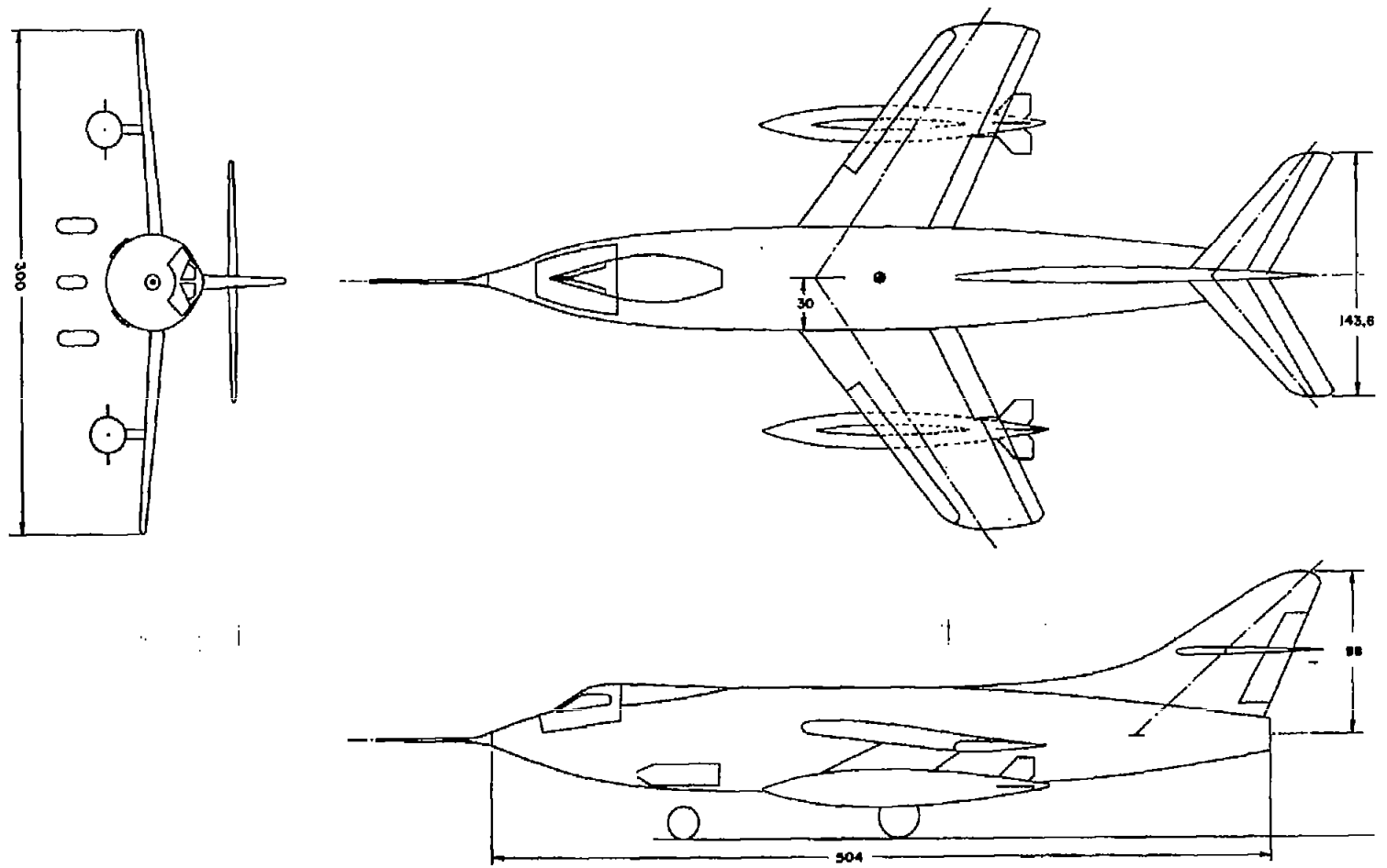

Figure 2.- General arrangement of the D-558-II airplane with 150-gallon stores at the 61-percent-wing semispan. All dimensions in inches.

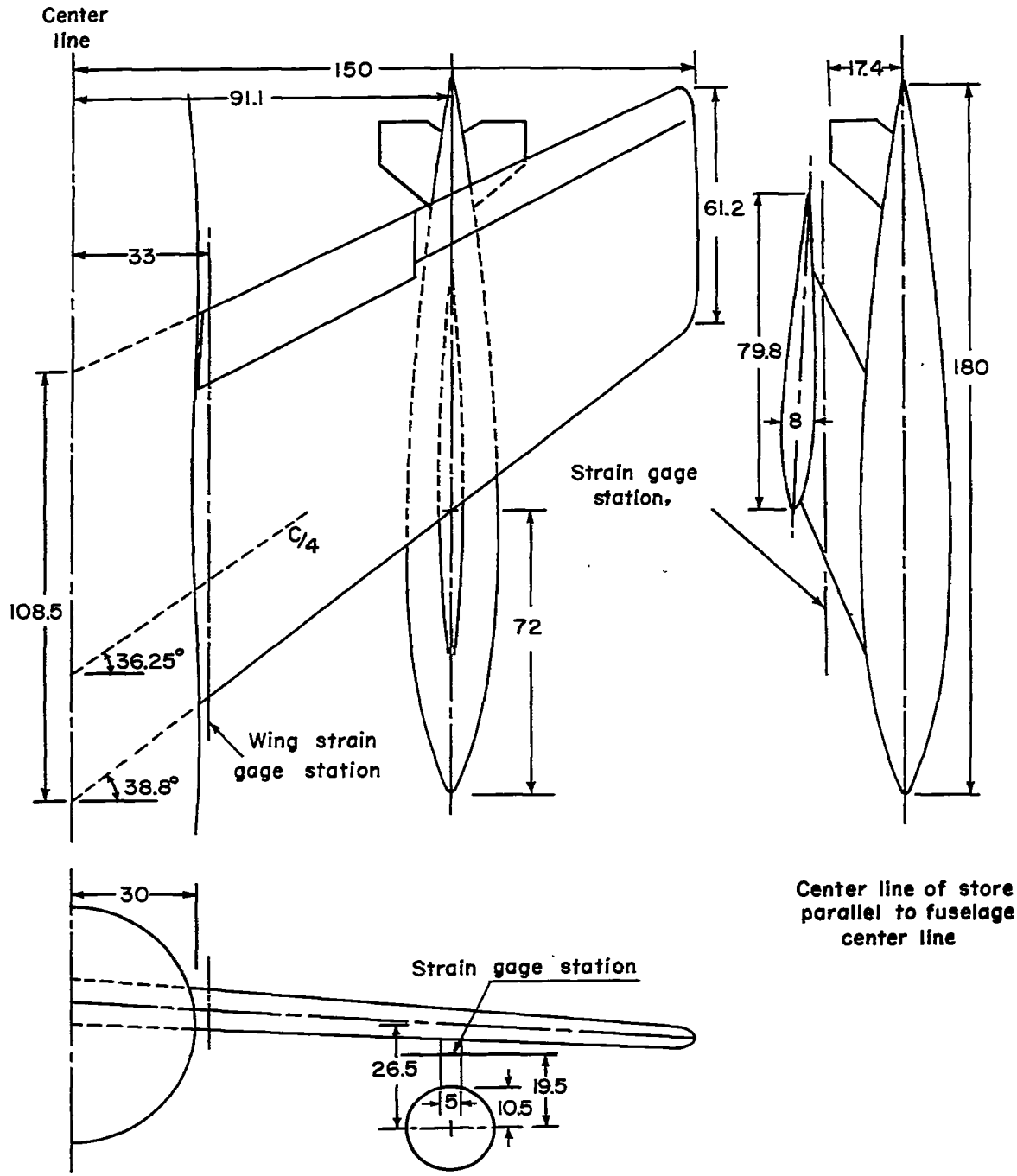

(a) Three-view scale drawing of the external-store installation.

Figure 3.- Detailed drawings of external store and fin. All dimensions in inches.

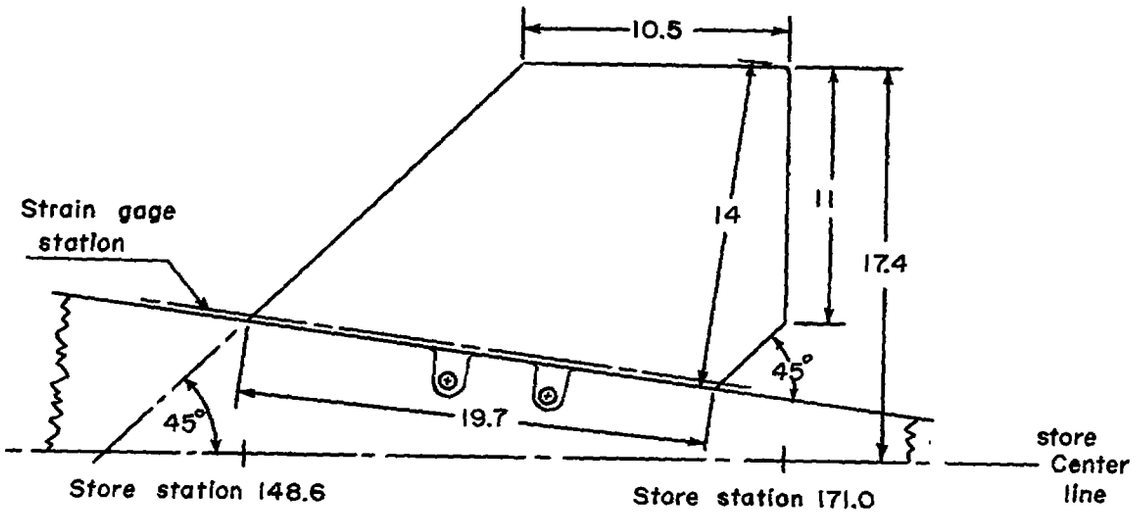

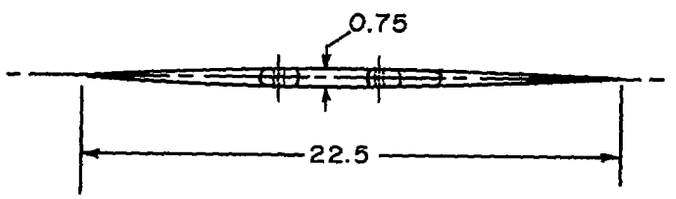

(b) Two-view scale drawing of a typical external-store fin.

Figure 3.- Concluded.

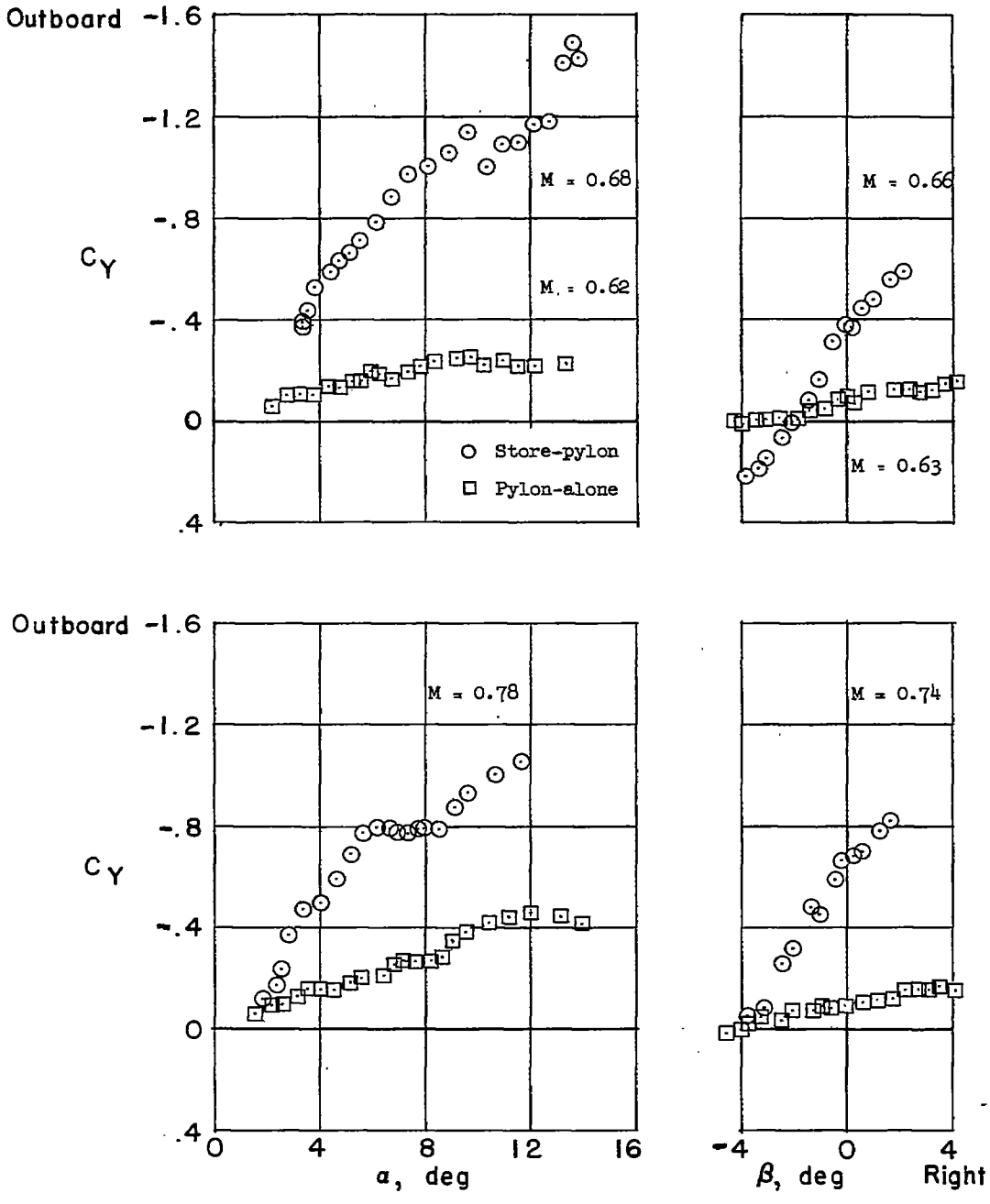

(a) Subsonic Mach numbers.

Figure 4.- Variation of the external-store and pylon side-force coefficient with angle of attack and sideslip for several representative Mach numbers.

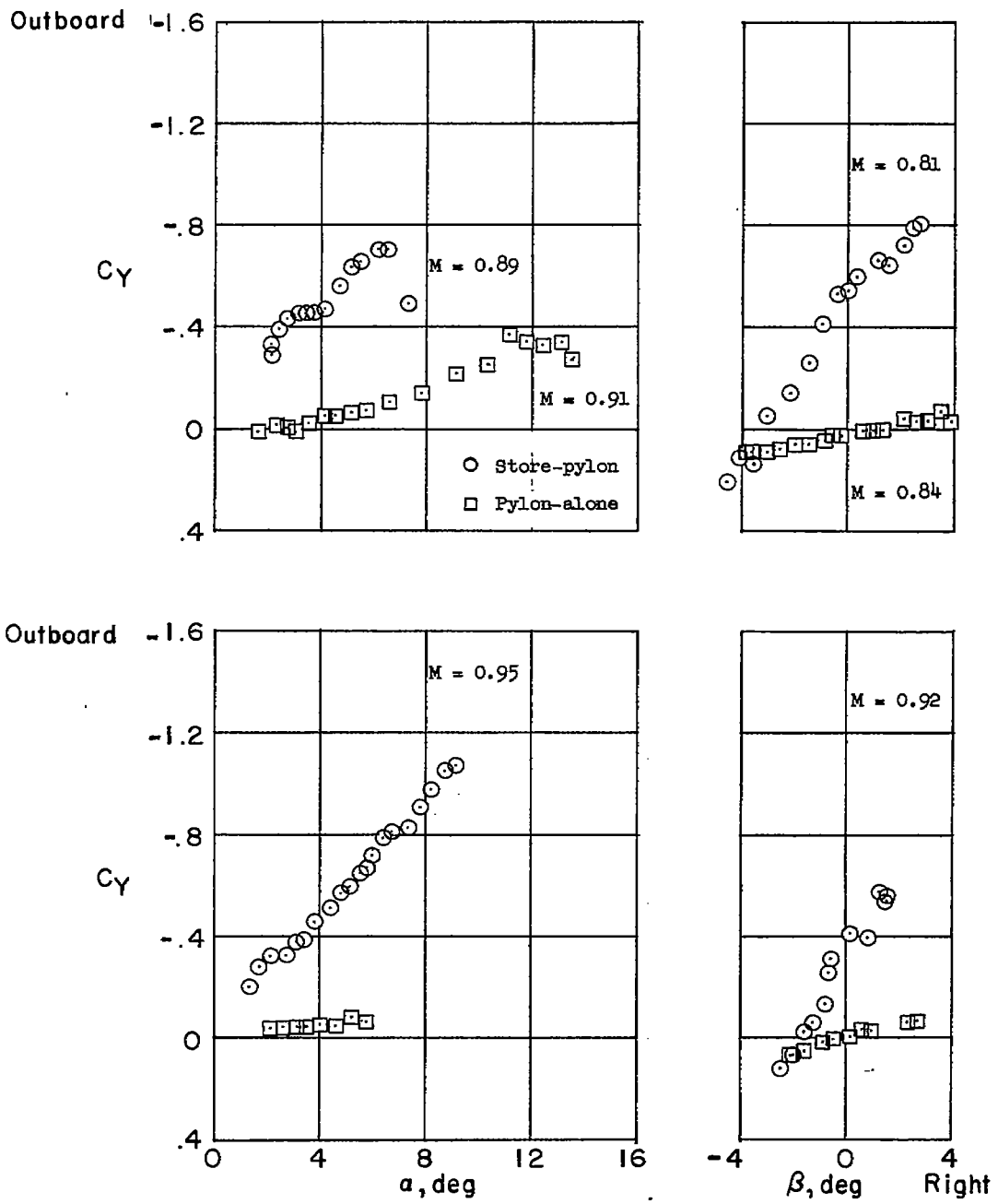

(b) Transonic Mach numbers.

Figure 4.- Continued.

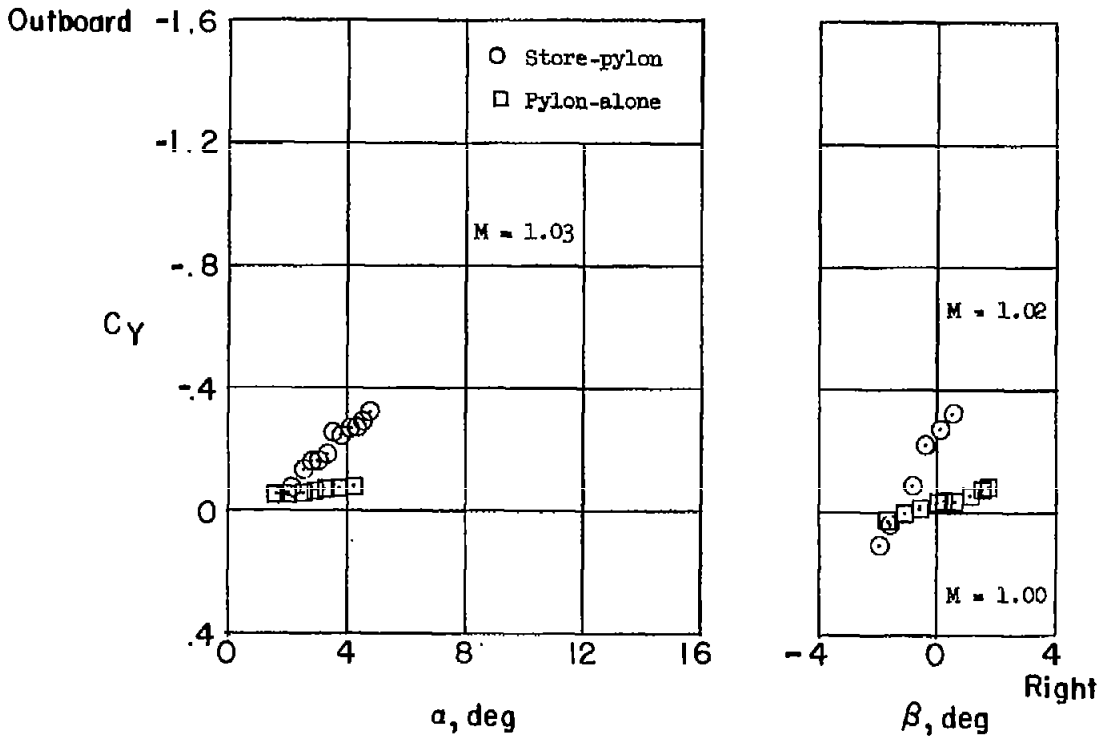

(c) Supersonic Mach numbers.

Figure 4.- Concluded.

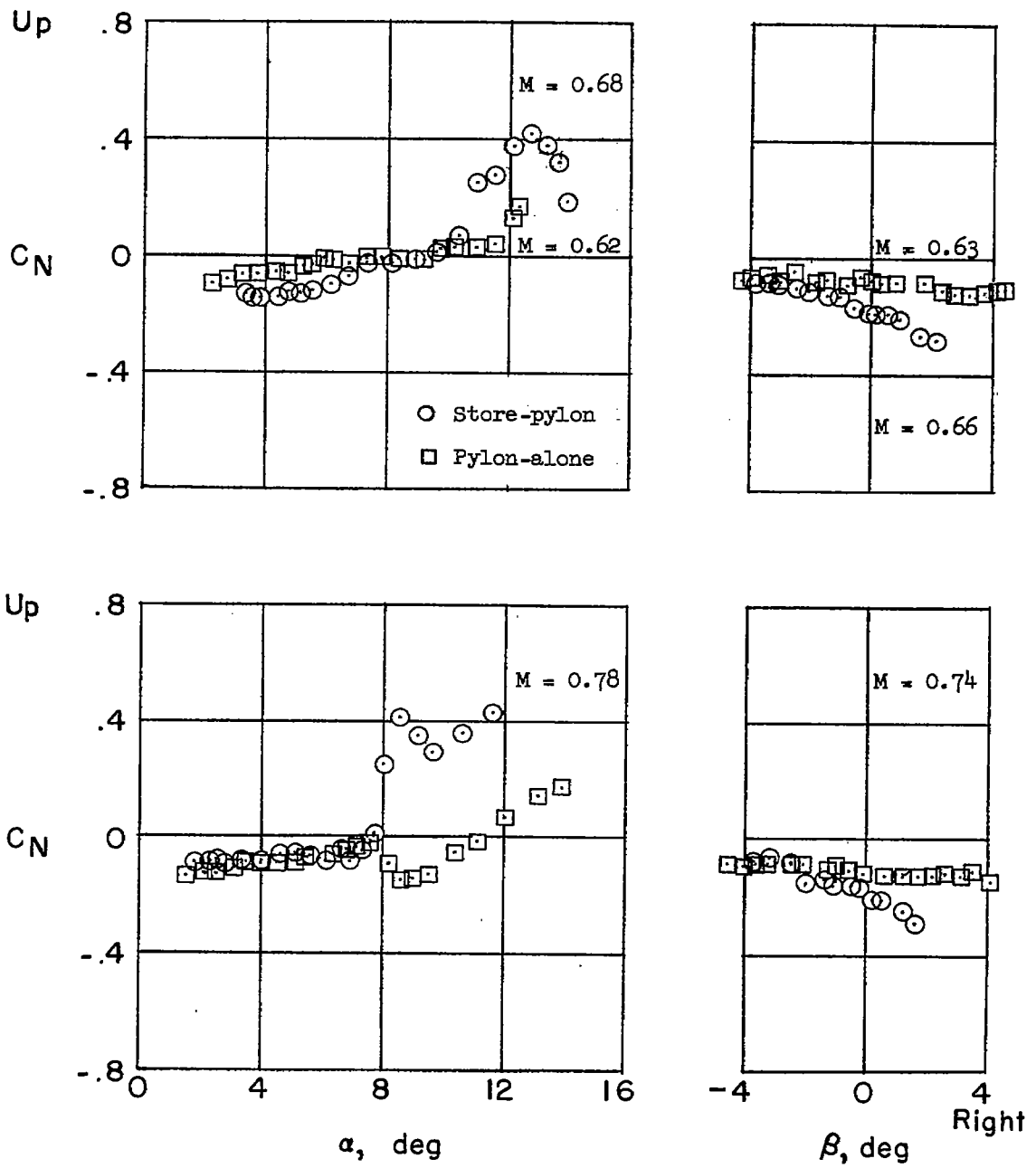

(a) Subsonic Mach numbers.

Figure 5.- Variation of the external-store and pylon normal-force coefficient with angle of attack and sideslip for several representative Mach numbers.

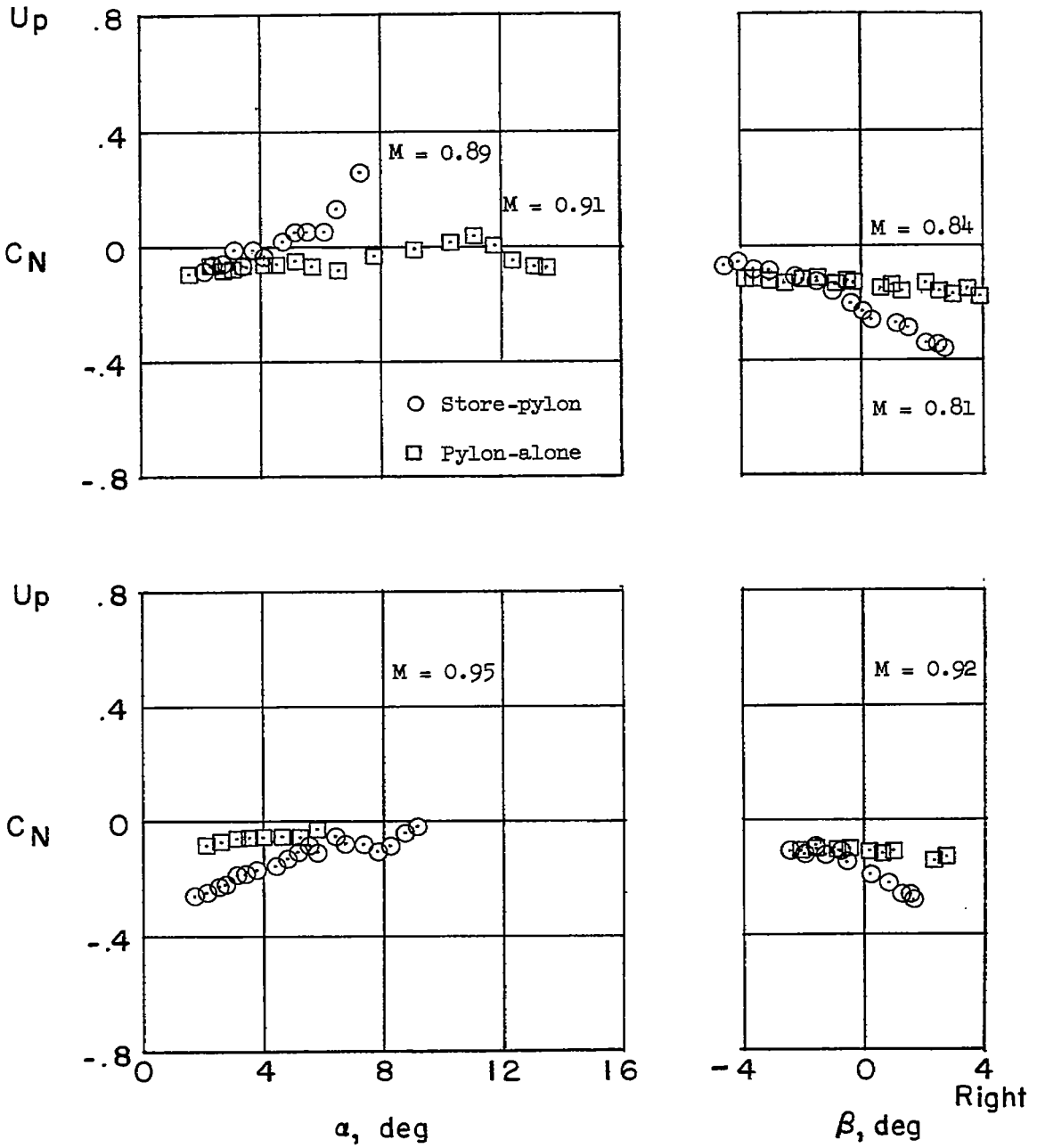

(b) Transonic Mach numbers.

Figure 5.- Continued.

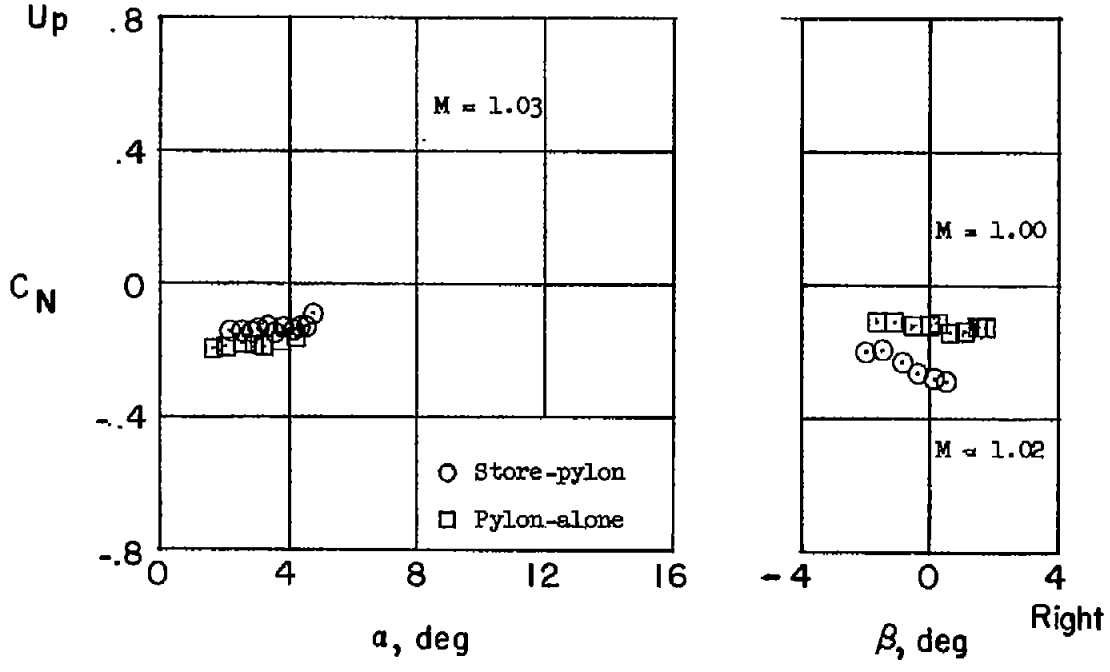

(c) Supersonic Mach numbers.

Figure 5.- Concluded.

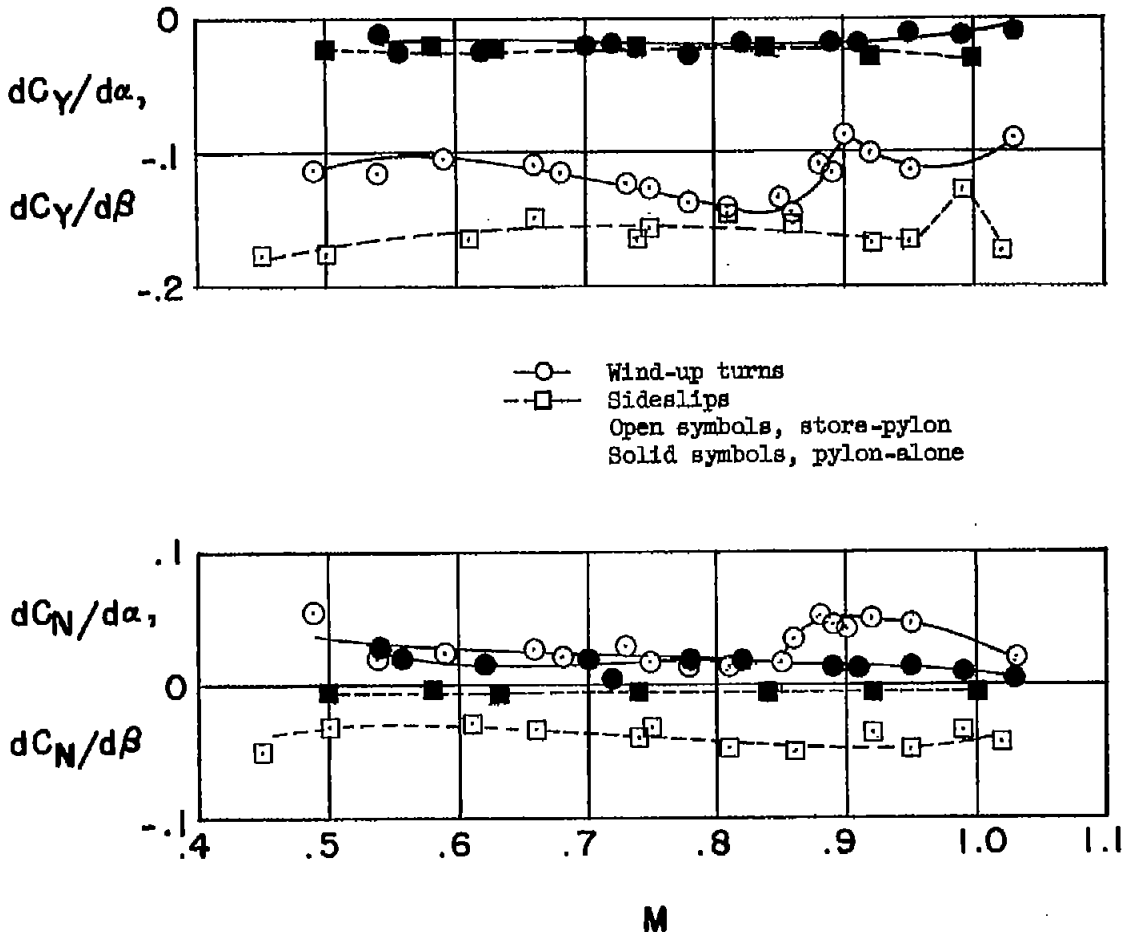

Figure 6.- Variation with Mach number of the side-force- and normal-force-load-coefficient slopes.

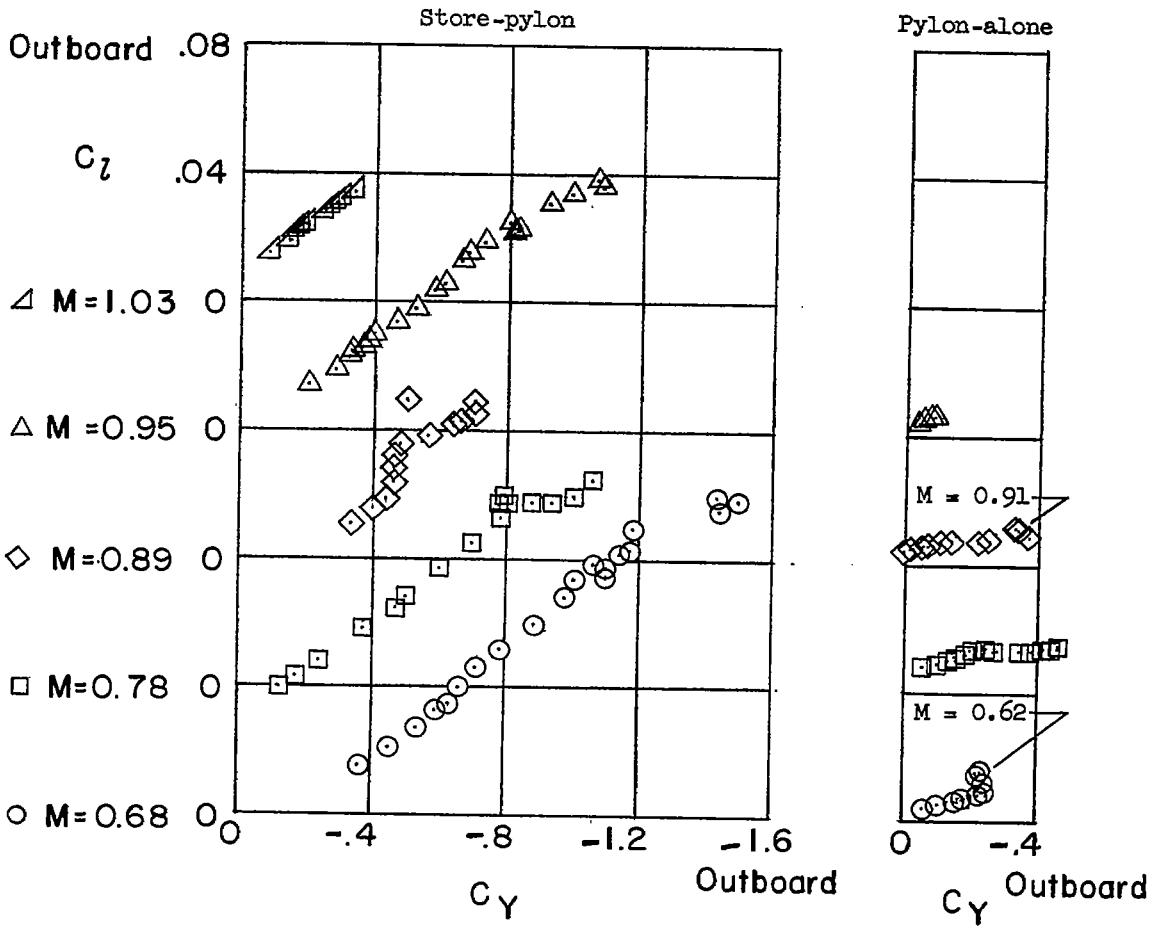

(a) Angle-of-attack maneuvers.

Figure 7.- Variation of the store-pylon and pylon-alone rolling-moment coefficient with side-force coefficient for several representative Mach numbers.

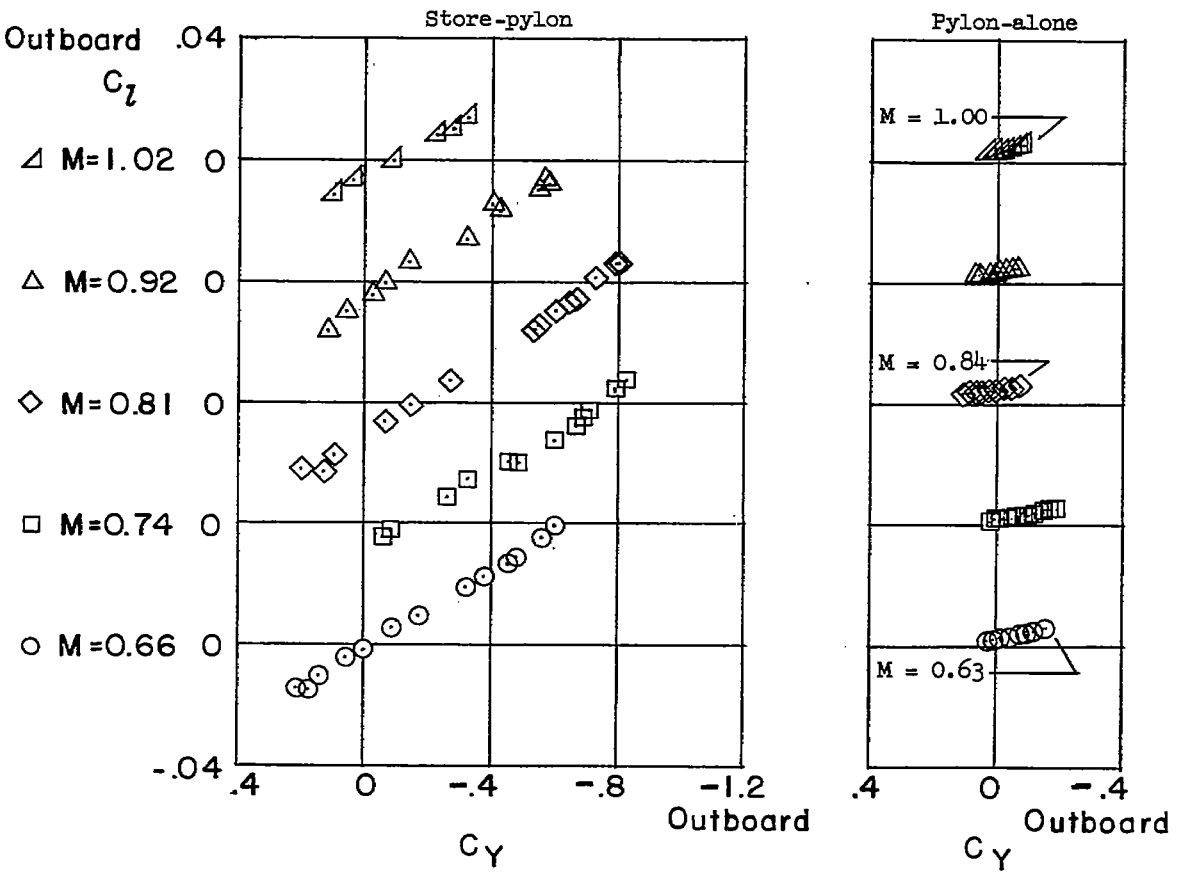

(b) Sideslip maneuvers.

Figure 7.- Concluded.

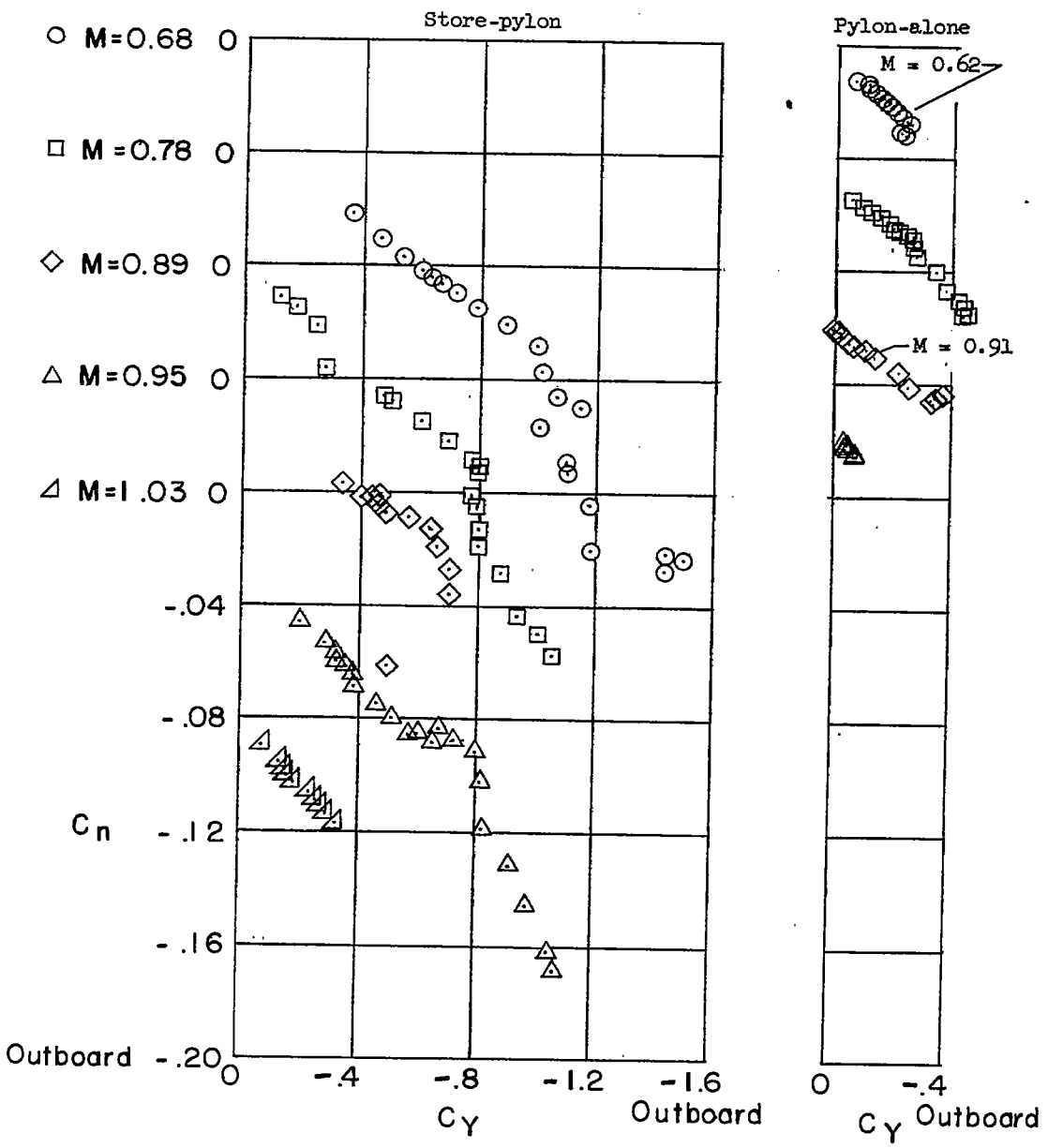

(a) Angle-of-attack maneuvers.

Figure 8.- Variation of the store-pylon and pylon-alone yawing-moment coefficient with side-force coefficient for several representative Mach numbers.

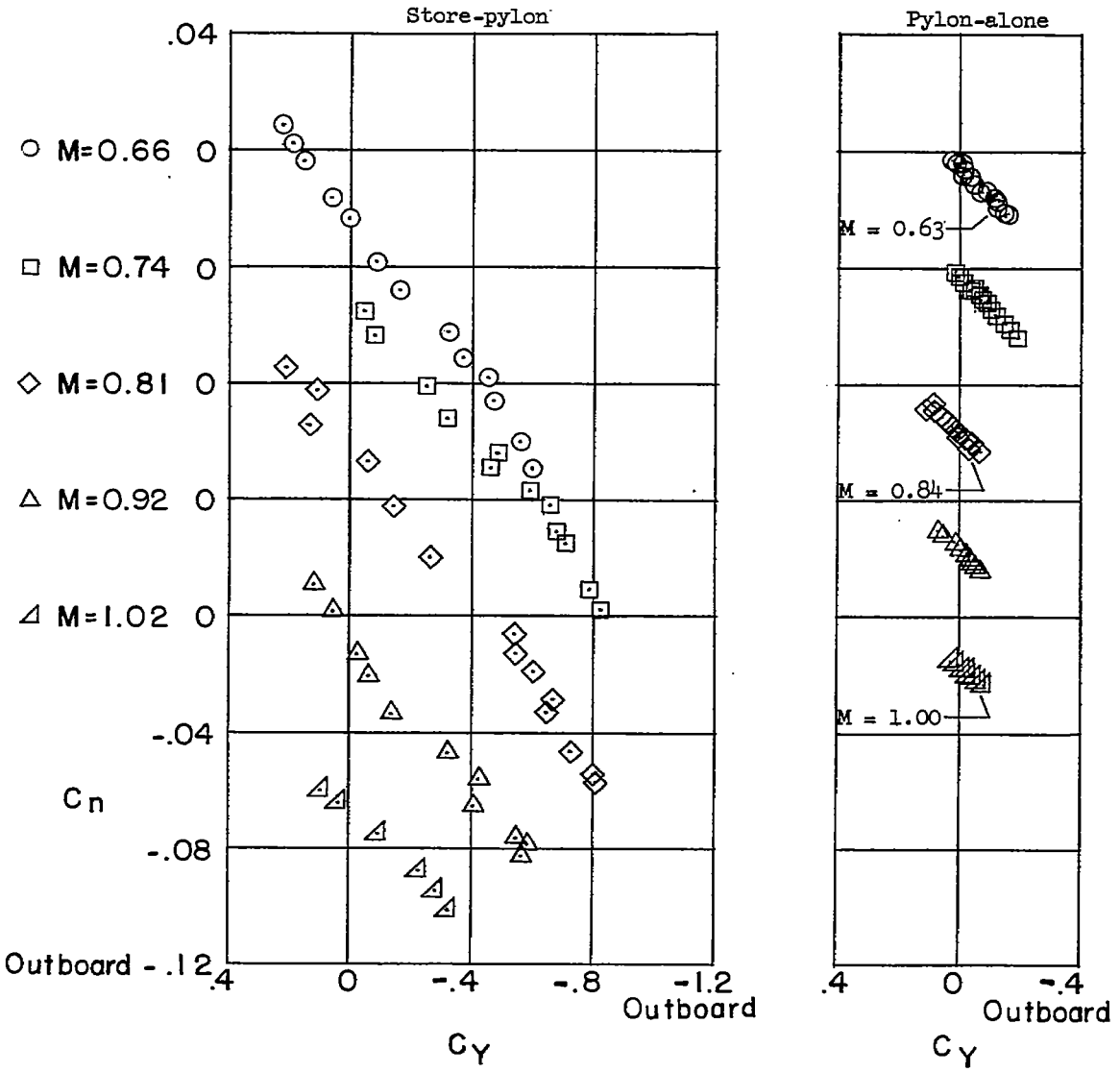

(b) Sideslip maneuvers.

Figure 8.- Concluded.

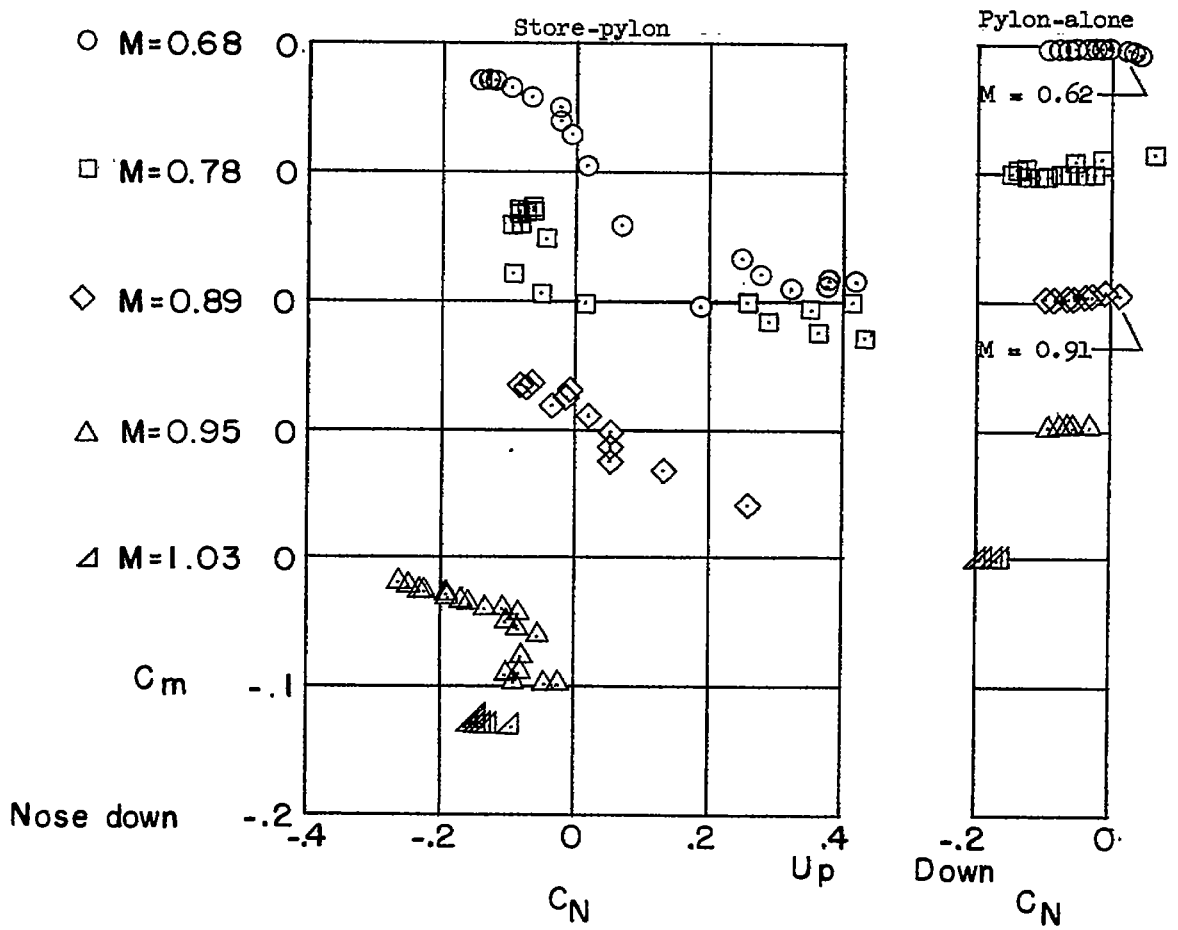

(a) Angle-of-attack maneuvers.

Figure 9.- Variation of the store-pylon and pylon-alone pitching-moment coefficient with normal-force coefficient for several representative Mach numbers.

[redacted]

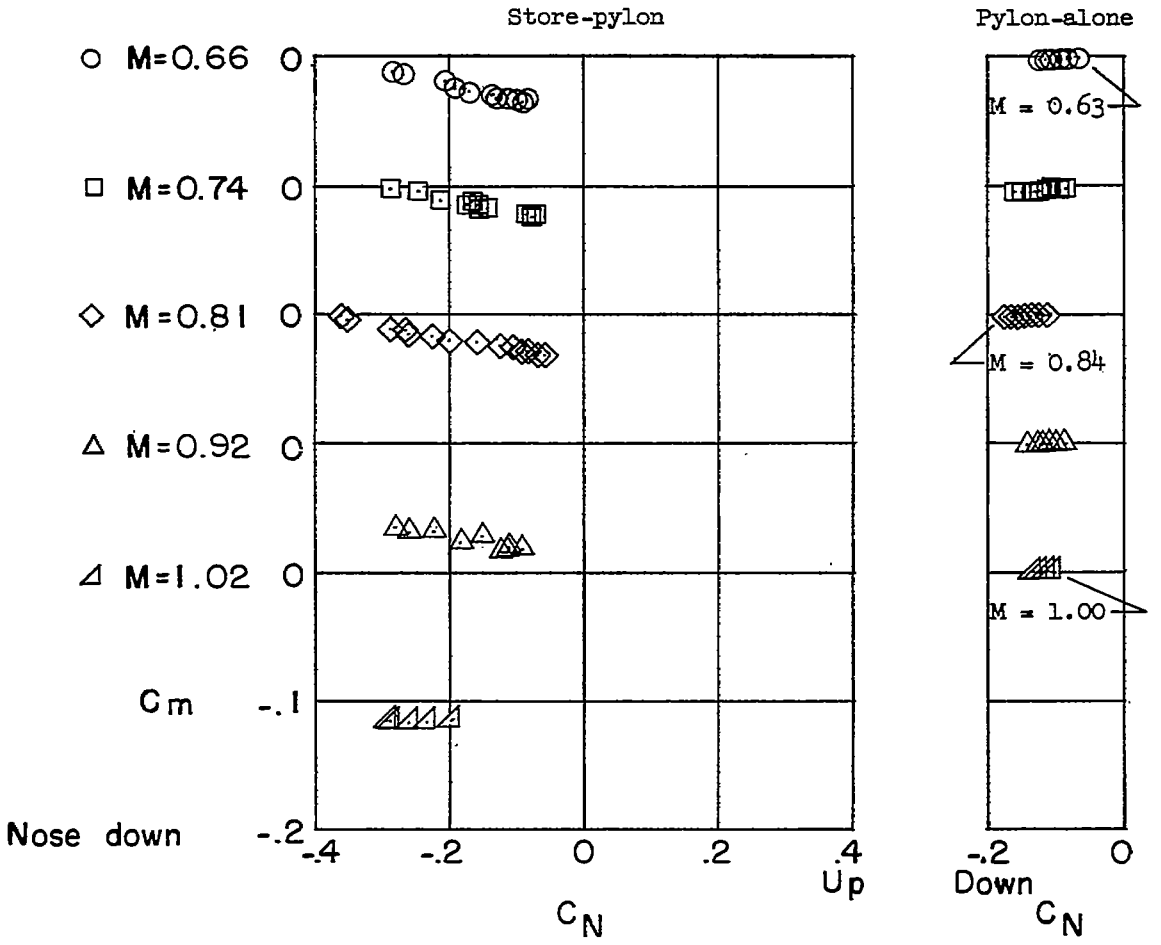

(b) Sideslip maneuvers.

Figure 9.- Concluded.

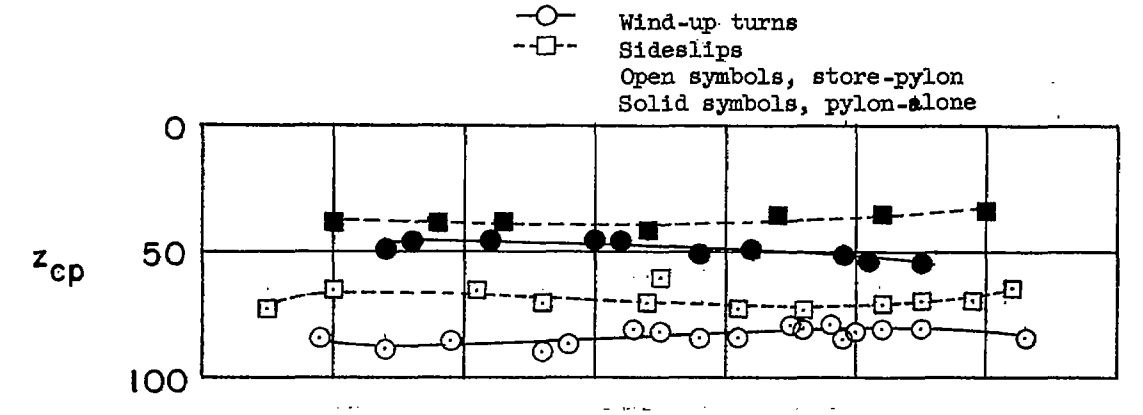

(a) Vertical center of pressure due to side force.

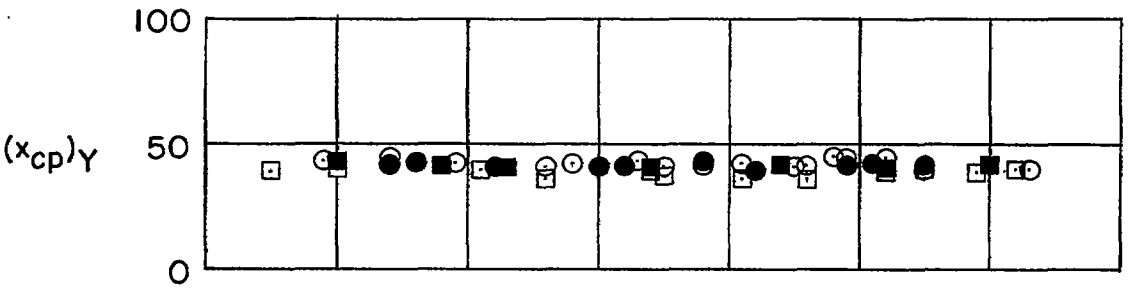

(b) Longitudinal center of pressure due to side force.

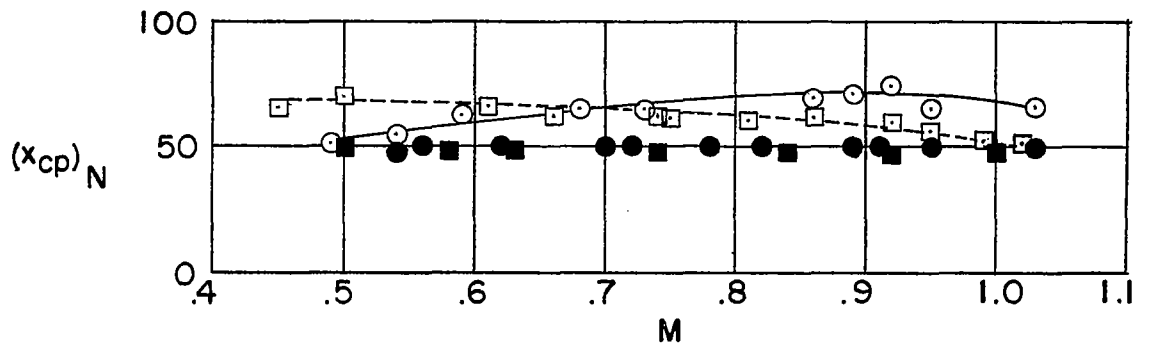

(c) Longitudinal center of pressure due to normal force.

Figure 10.- Variation of the store and pylon centers of pressure of the additional airload with Mach number.

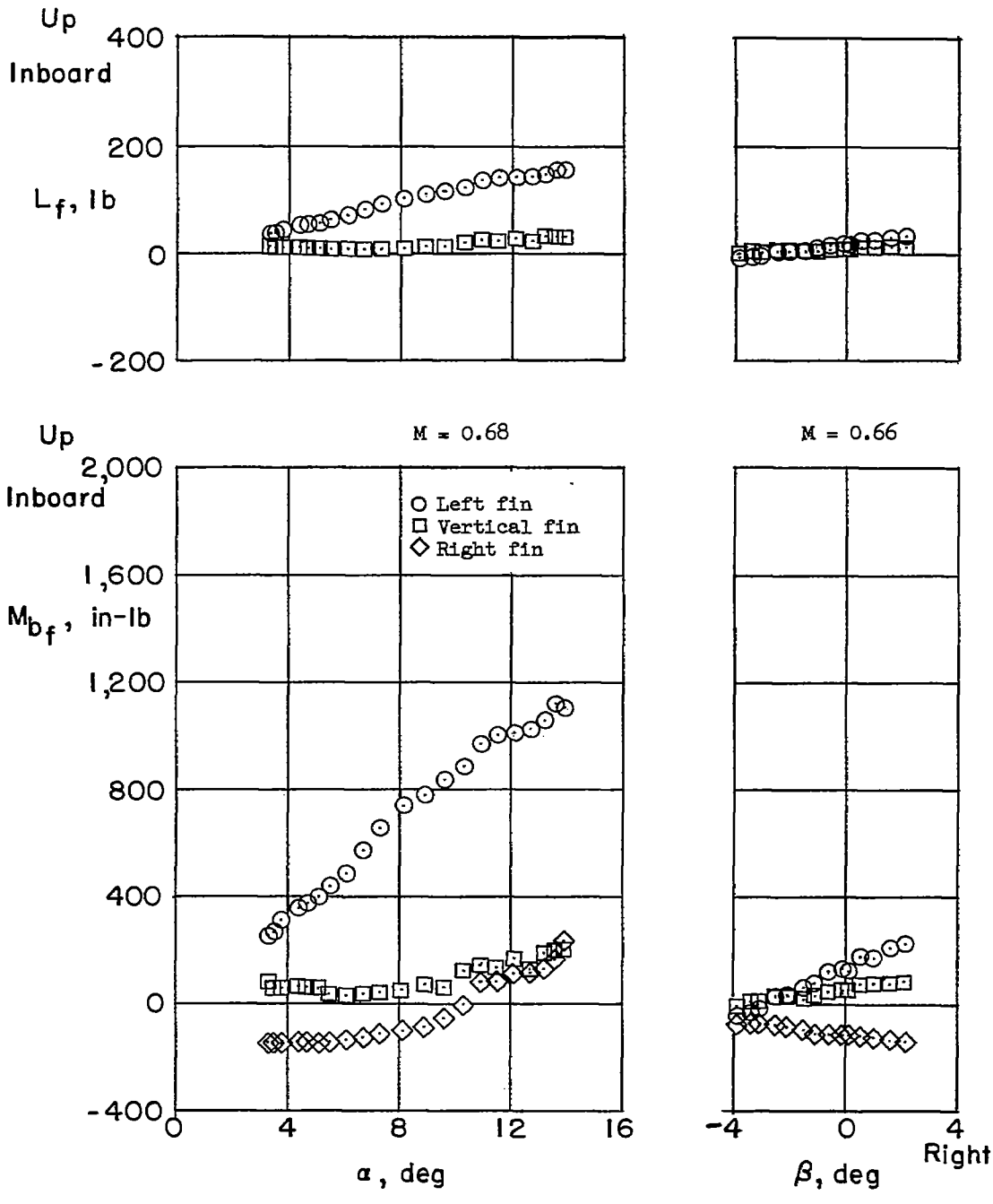

(a) Subsonic Mach numbers.

Figure 11.- Variation of the external-store fin loads and moments with angle of attack and sideslip for several representative Mach numbers.

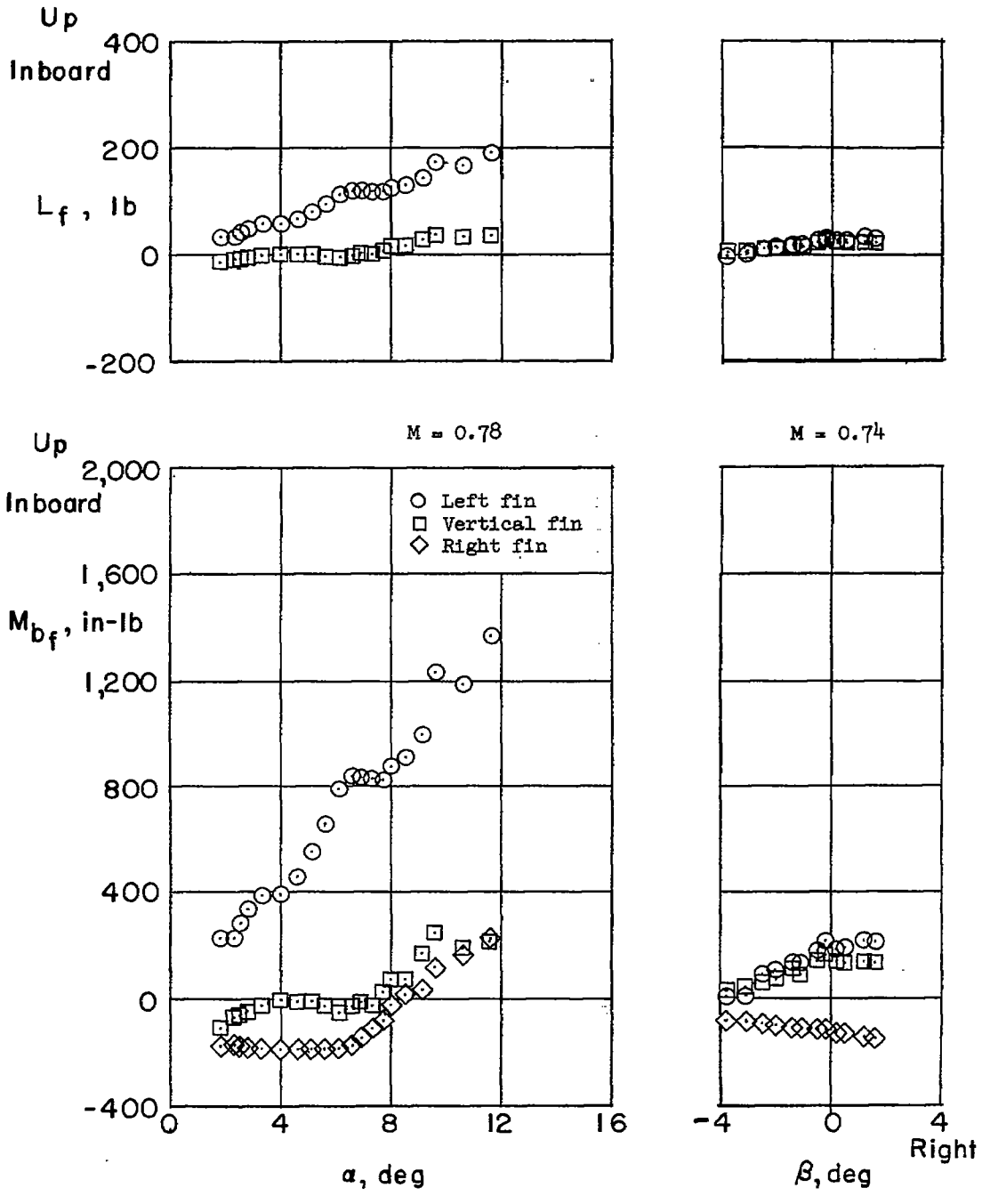

(b) Subsonic Mach numbers.

Figure 11.- Continued.

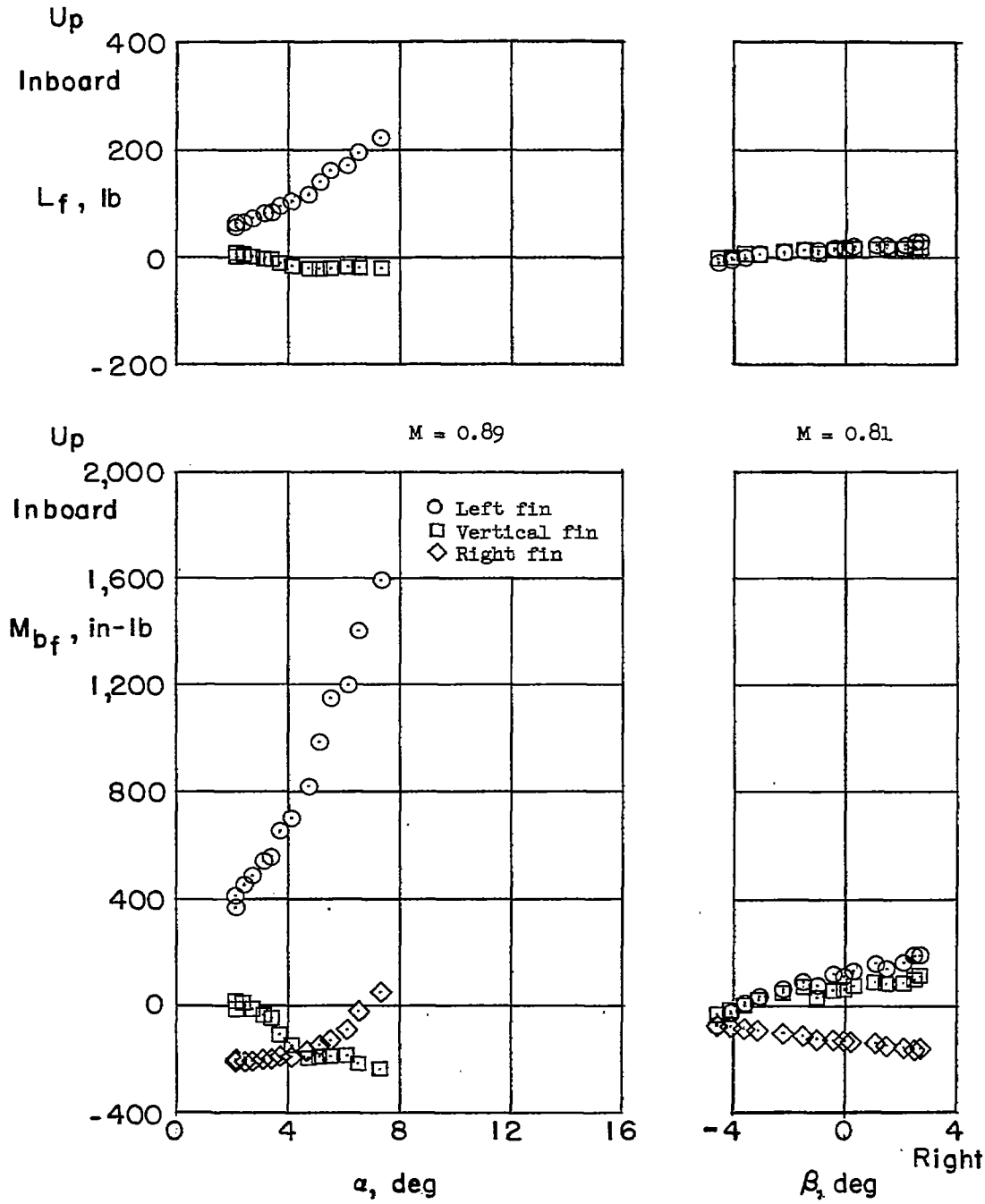

(c) Transonic Mach numbers.

Figure 11.- Continued.

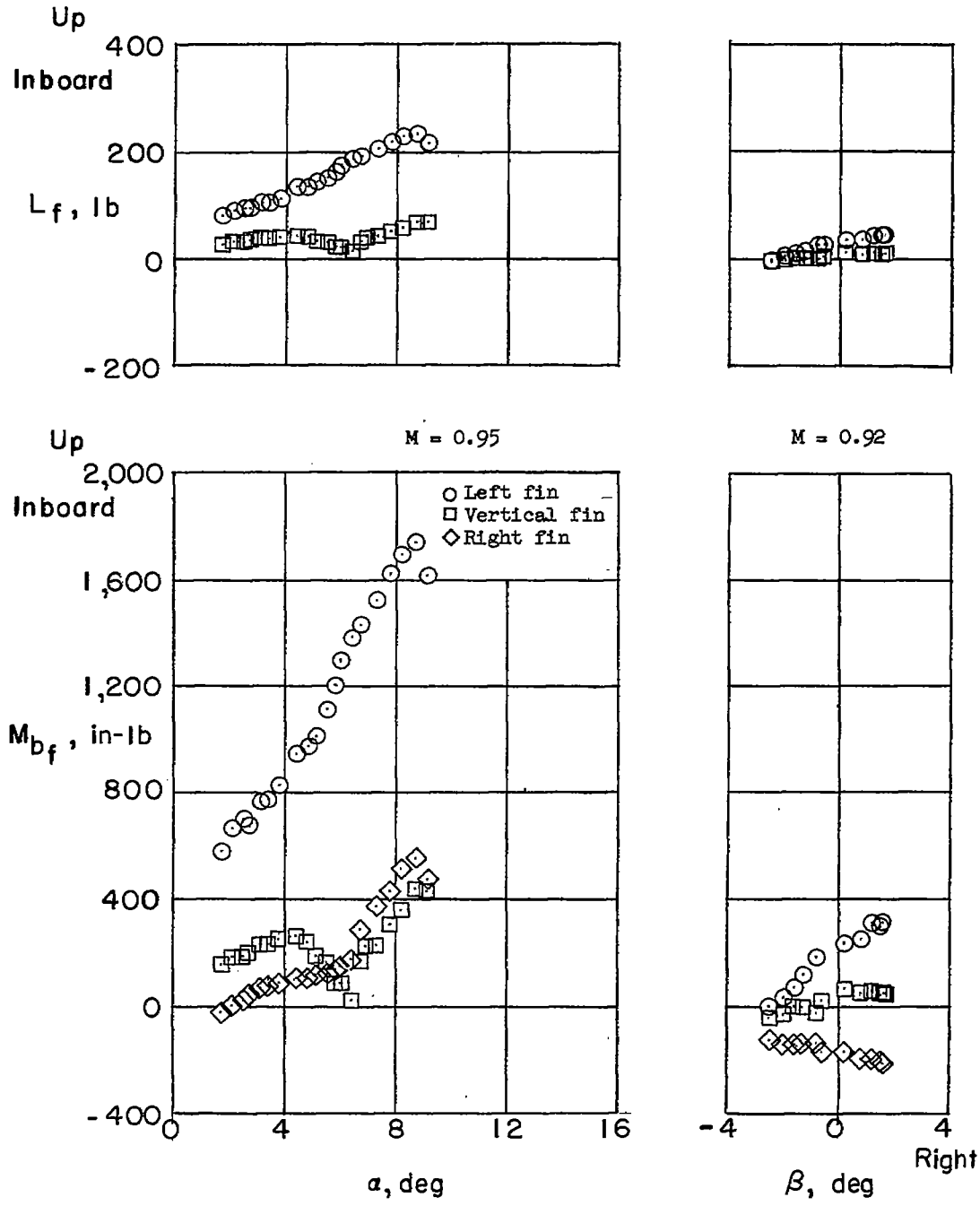

(d) Transonic Mach numbers.

Figure 11.- Continued.

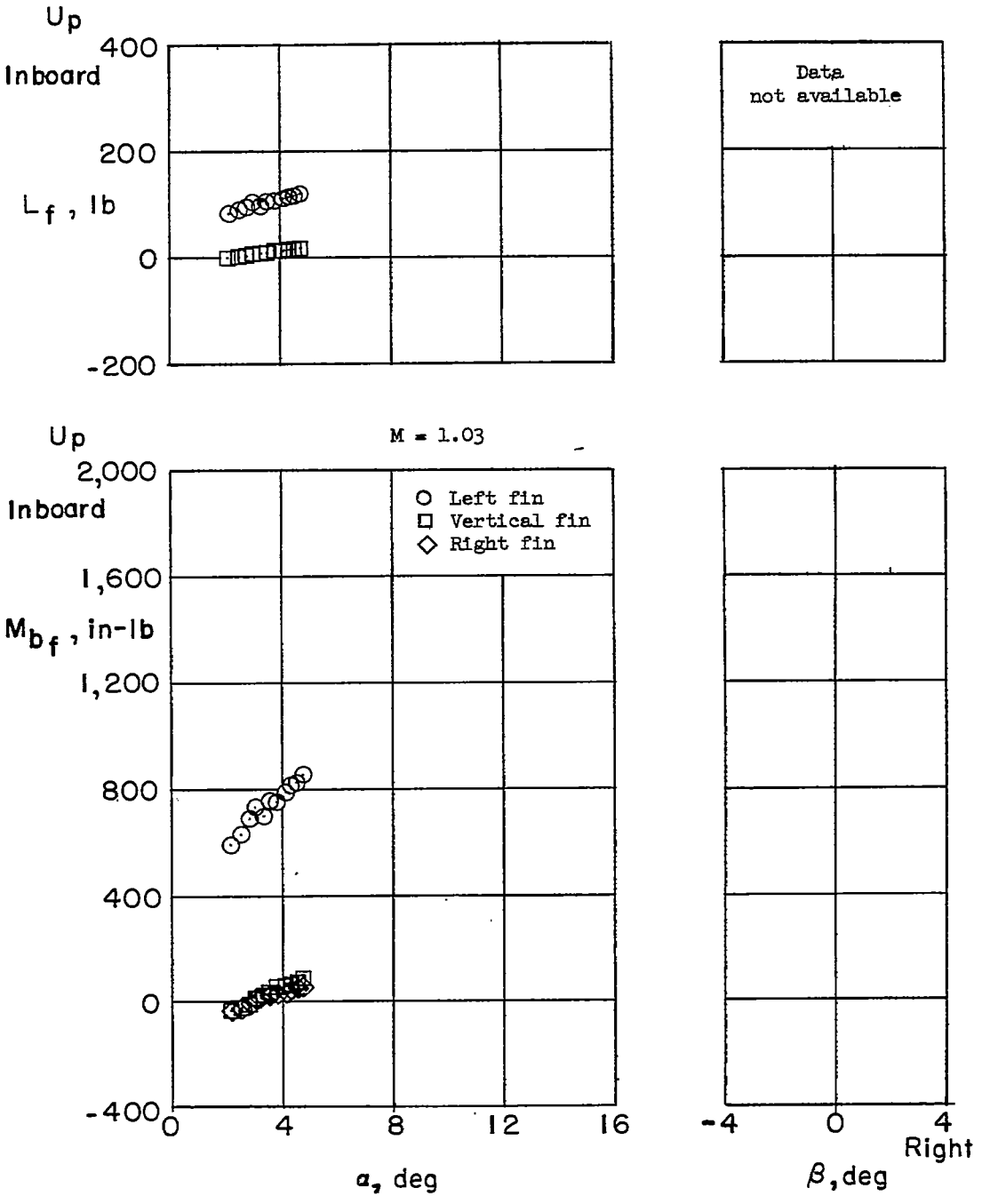

(e) Supersonic Mach numbers.

Figure 11.- Concluded.

[redacted]

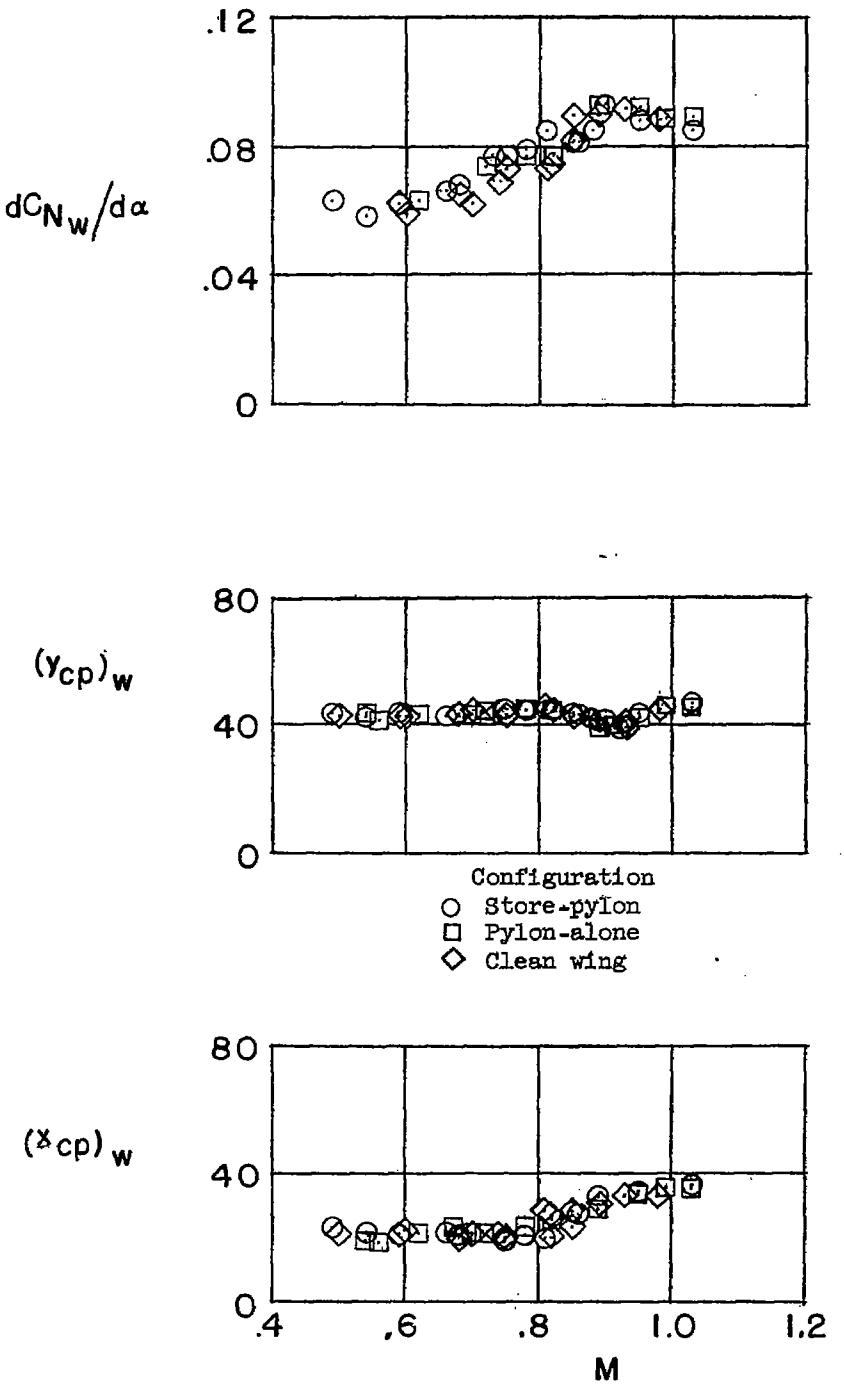

Figure 12.- Variation of the left wing-panel-load parameters with Mach number.